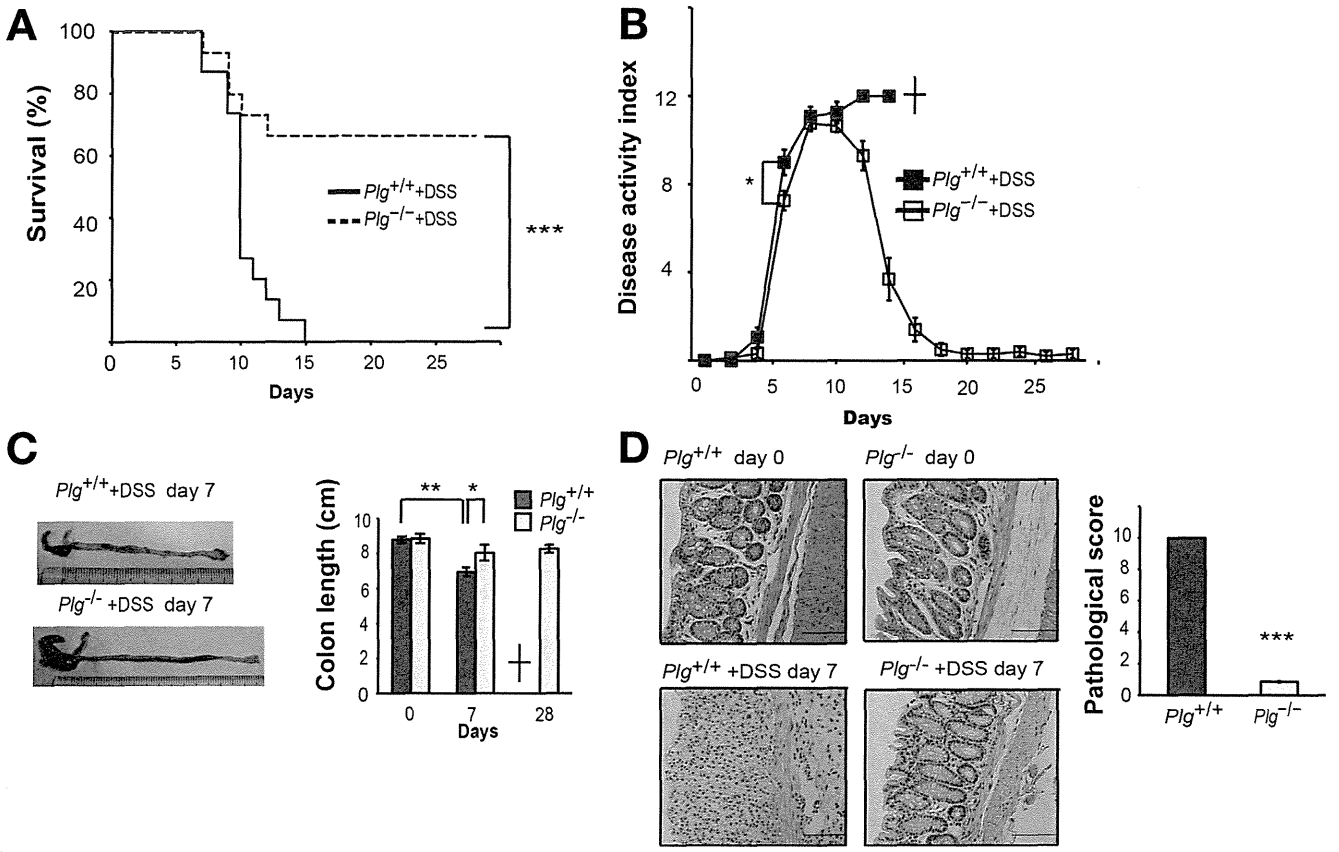

Figure 3. *Plg*-deficient mice are less susceptible to DSS-induced colitis. (*A*) Survival and (*B*) DAI were determined over the indicated time period in DSS-treated $Plg^{+/+}$ and $Plg^{-/-}$ mice: $n = 15$/group. (*C*) $Plg^{-/-}$ mice show shorter colon lengths. $n = 9$ for each group. *Right*: Representative H&E-stained colon sections from DSS-treated $Plg^{+/+}$ and $Plg^{-/-}$ mice. *Scale bars*: 200 μm. n = 3/group for all experiments. (*D*) *Right*: Pathologic scores obtained using colon tissues. Values represent means ± SEM. The percentage of survival was determined. n = 3. $^{*}P < .05$, $^{**}P < .01$, and $^{***}P < .001$, determined by a 2-tailed Student *t* test and log-rank test.

IL), and antifibrinogen Ab (Biogenesis, Poole, United Kingdom) followed by donkey anti-rat IgG Ab conjugated with 594, donkey anti-rabbit, or goat IgG Ab conjugated with Alexa 488 and streptavidin–Alexa 488 (Invitrogen, Carlsbad, CA). Nuclei were stained using 4′,6-diamidino-2-phenylindole.

Terminal Deoxynucleotidyl Transferase–Mediated Deoxyuridine Triphosphate Nick-End Labeling Assay

Apoptosis was detected using colon sections according to the instructions provided by the manufacturer of the TAC2 TdT Kit (Funakoshi, Tokyo, Japan).

Quantification of Cytokine Messenger RNA Expression in Colon Tissues by Reverse-Transcription Polymerase Chain Reaction

Total RNA was extracted using TRIzol (Invitrogen), and complementary DNA was generated according to the manufacturer's protocols. A total of 10 mg of colon was used. Peripheral blood mononuclear cells were isolated by centrifugation using Lympholyte (Cedarlane, Inc, Ontario, Canada). Polymerase chain reaction was performed with the following specific forward and reverse primer pairs, respectively: *Plau*: 5′-gtcctctctgcaacagagtc-3′ and 5′-ctgtgtctgagggtaatgct-3′; *Plat*: 5′-gtactgctttgtggact-3′ and 5′-tgctgttggtaagttgtctg-3′; *Tnf*: 5′-gccgatttgctatctcatac-3′ and

Figure 4. Plasmin-mediated prevention of colitis progression requires MMP9. (*A*) Representative immunohistochemical images of Gr-1/MMP9-stained colon tissue sections retrieved 7 days after DSS induction of C57BL/6 mice treated with or without YO-2. *Arrows* indicate positively stained cells. n = 3/group. (*B*) Blood serum samples and (*C*) culture supernatants derived from colon tissue of YO-2– or phosphate-buffered saline (PBS)-treated C57BL/6 mice were analyzed by gelatinolytic zymography (*left*). *Right*: Quantification of the proteolytic activity of MMP2 and MMP9 were detected by densitometry. n = 5/group. (*D*) Survival was determined in DSS-induced colitic $Mmp9^{-/-}$ and wild-type mice injected with YO-2 or MMI270. Values represent means ± SEM. Survival was determined in the following treatment groups: $Mmp9^{+/+}$ + PBS and $Mmp9^{+/+}$ + YO-2, n = 15; $Mmp9^{-/-}$ + PBS and $Mmp9^{-/-}$ + YO-2, n = 15; $Mmp9^{+/+}$ + MMP270 and $Mmp9^{-/-}$ + MMP270, n = 20. (*E*) DAI and representative H&E-stained colon sections (*F*) from DSS-treated $Mmp9^{+/+}$ and $Mmp9^{-/-}$ colitic mice (*right panel*) are shown. *Scale bars*: 200 μm. n = 3/group for all experiments. $^{*}P < .05$, $^{**}P < .01$, and $^{***}P < .001$, determined by a 2-tailed Student *t* test and log-rank test. CTL, control day 0.

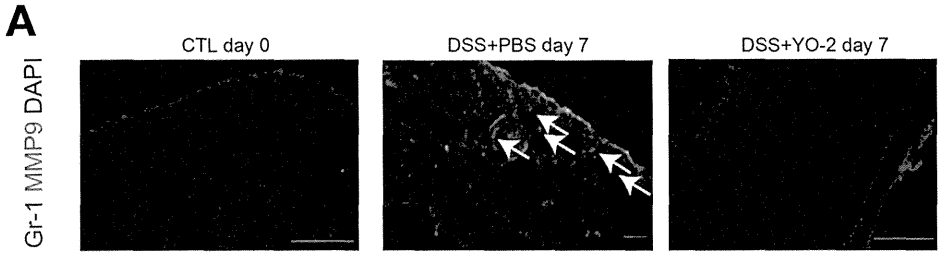
A
CTL day 0
DSS+PBS day 7
DSS+YO-2 day 7
Gr-1 MMP9 DAPI

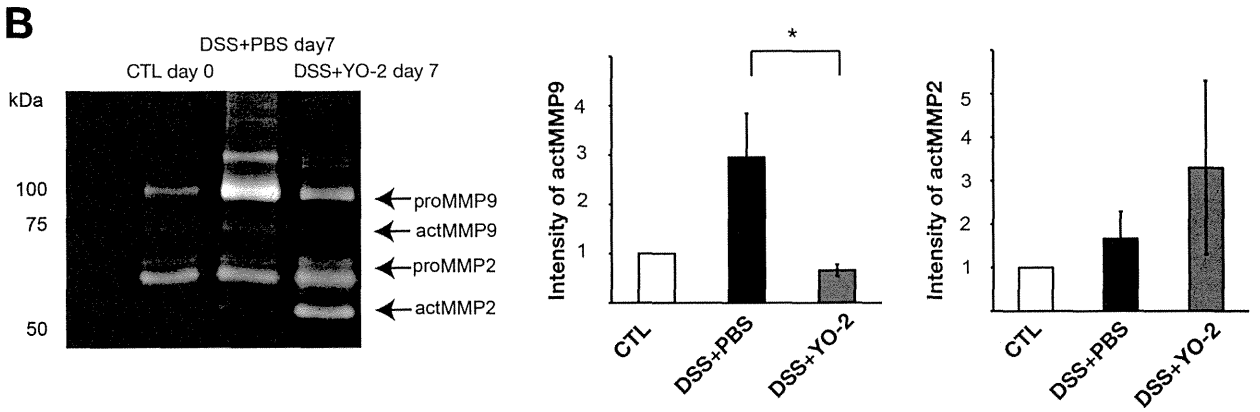
B
DSS+PBS day7
CTL day 0
DSS+YO-2 day 7
kDa
100
75
50
proMMP9
actMMP9
proMMP2
actMMP2
Intensity of actMMP9
Intensity of actMMP2
CTL
DSS+PBS
DSS+YO-2

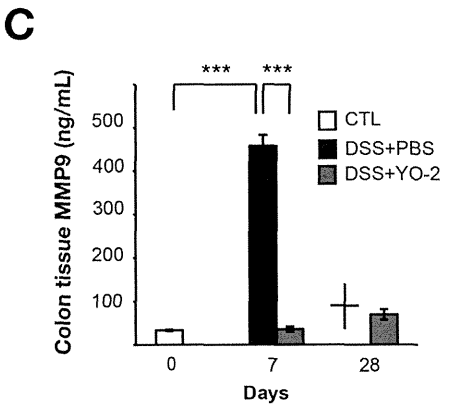
C
Colon tissue MMP9 (ng/mL)
CTL
DSS+PBS
DSS+YO-2
Days

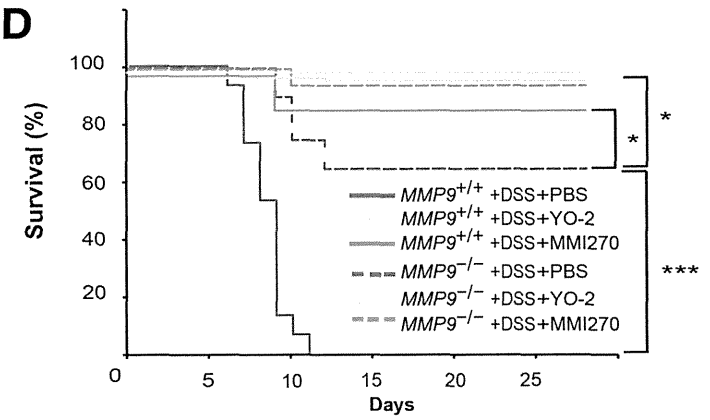
D
Survival (%)
MMP9+/+ +DSS+PBS
MMP9+/+ +DSS+YO-2
MMP9+/+ +DSS+MMI270
MMP9−/− +DSS+PBS
MMP9−/− +DSS+YO-2
MMP9−/− +DSS+MMI270
Days

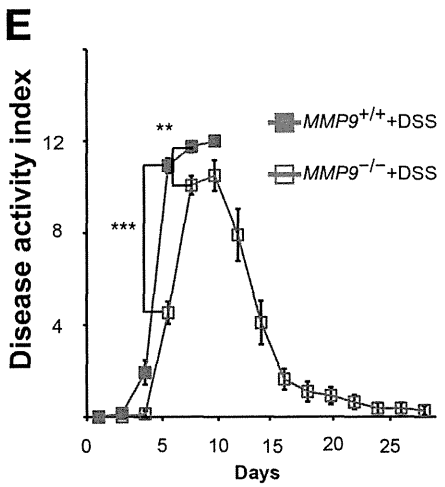
E
Disease activity index
MMP9+/+ +DSS
MMP9−/− +DSS
Days

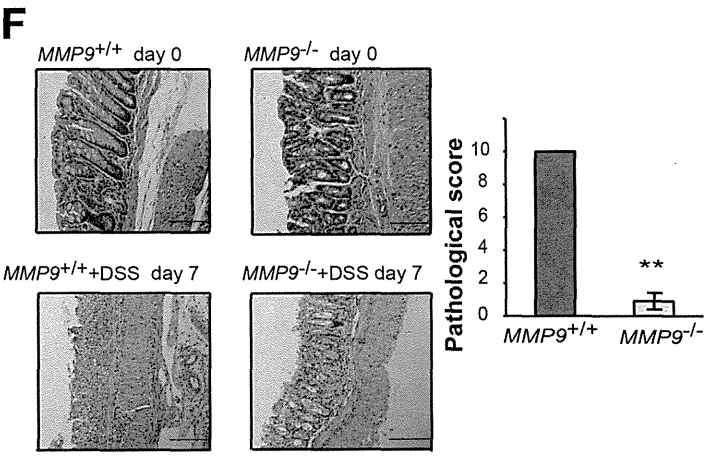
F
MMP9+/+ day 0
MMP9−/- day 0
MMP9+/+ +DSS day 7
MMP9−/-+DSS day 7
Pathological score
MMP9+/+
MMP9−/-

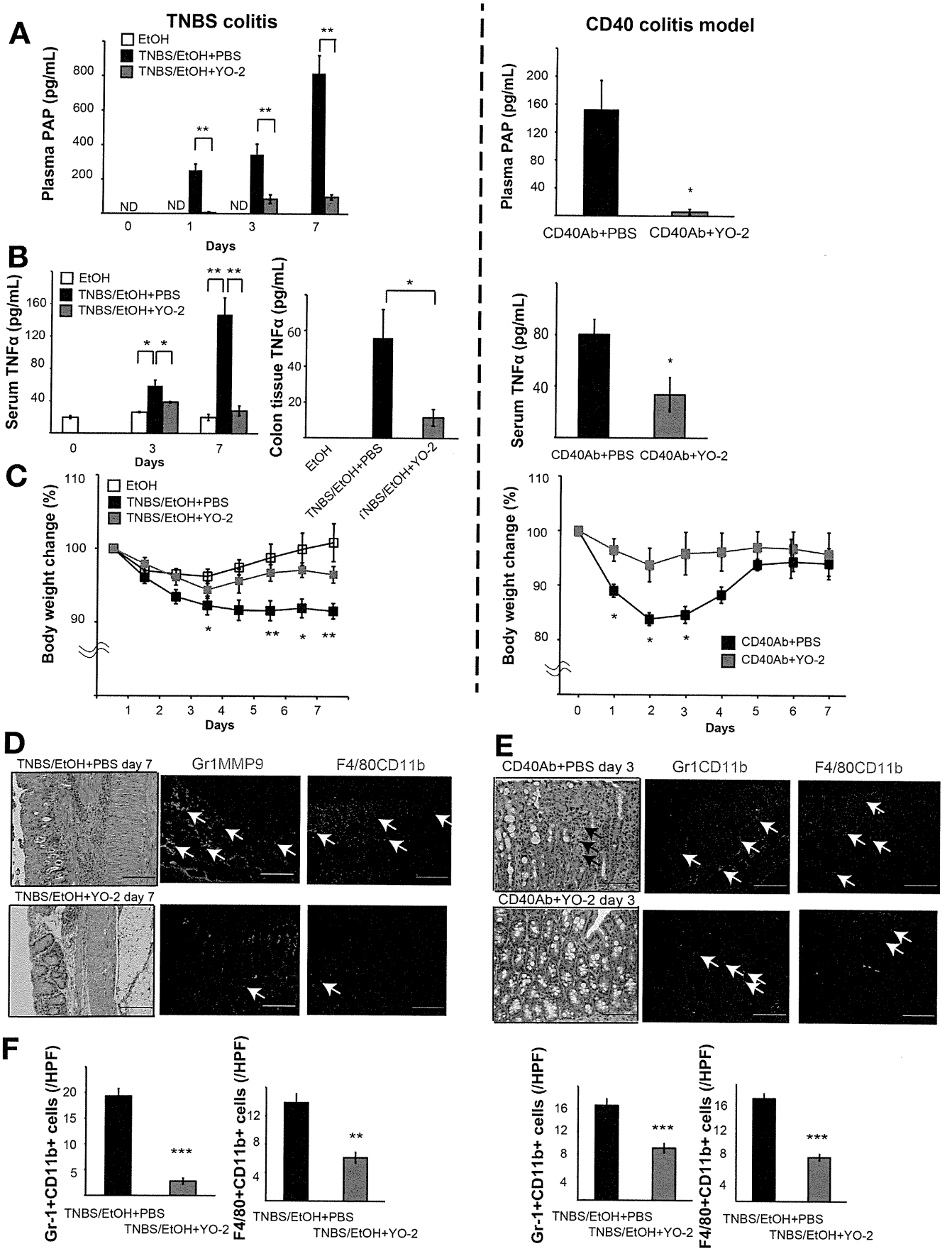
A
TNBS colitis
EtOH
TNBS/EtOH+PBS
TNBS/EtOH+YO-2
Plasma PAP (pg/mL)
800
600
400
200
ND
ND
ND
0
1
3
7
Days
**
**
**
CD40 colitis model
Plasma PAP (pg/mL)
200
160
120
80
40
CD40Ab+PBS
CD40Ab+YO-2
B
Serum TNFα (pg/mL)
160
120
80
40
0
3
7
Days
Colon tissue TNFα (pg/mL)
60
40
20
EtOH
TNBS/EtOH+PBS
TNBS/EtOH+YO-2
Serum TNFα (pg/mL)
80
40
CD40Ab+PBS
CD40Ab+YO-2
C
Body weight change (%)
110
100
90
1
2
3
4
5
6
7
Days
Body weight change (%)
110
100
90
80
0
1
2
3
4
5
6
7
Days
CD40Ab+PBS
CD40Ab+YO-2
D
TNBS/EtOH+PBS day 7
Gr1MMP9
F4/80CD11b
TNBS/EtOH+YO-2 day 7
E
CD40Ab+PBS day 3
Gr1CD11b
F4/80CD11b
CD40Ab+YO-2 day 3
F
Gr-1+CD11b+ cells (/HPF)
20
15
10
5
***
TNBS/EtOH+PBS
TNBS/EtOH+YO-2
F4/80+CD11b+ cells (/HPF)
12
8
4
**
TNBS/EtOH+PBS
TNBS/EtOH+YO-2
Gr-1+CD11b+ cells (/HPF)
16
12
8
4
***
TNBS/EtOH+PBS
TNBS/EtOH+YO-2
F4/80+CD11b+ cells (/HPF)
16
12
8
4
***
TNBS/EtOH+PBS
TNBS/EtOH+YO-2

5'-ggtatatgggctcataccag-3'; *Il1b*: 5'-gcaactgttcctgaactc-3' and 5'-ctcggagcctgtagtgca-3'; *Il6*: 5'-tgacaggatgcagaaggaga-3' and 5'-gctggaaggtggacagtgag-3'; *Cxcl5*: 5'-gcatttctgttgctgttcacgctg-3' and 5'-cctccttctggtttttcagtttagc-3'; *Actb* control: 5'-gtatgaa-caacgatgatg-3' and 5'-ccagaagaccagaggaaa -3'.

Immunoassay

The levels of cytokines were determined in plasma, serum, and colon supernatants. Colon supernatants were prepared as described previously.[20] Samples were measured using mouse-specific enzyme-linked immunosorbent assay kits for murine MMP9, CXCL5, TNF-α (all R&D Systems), plasmin-antiplasmin complex (PAP) (Cusabio Biotech, Newark, DE), fibrin degradation product (FDP) (Uscn Life Science, Inc, Wuhan, China), thrombin–antithrombin (Abcam, Cambridge, MA), and interleukin (IL)1β and IL6 (Biolegend, San Diego, CA).

Gelatin Zymography

Plasma samples were treated with 20 μL gelatin-agarose beads at 4°C overnight and processed through sodium dodecyl sulfate–polyacrylamide gel electrophoresis acrylamide gels containing 1 mg/mL^{-1} gelatin. For more detail see the article by Heissig et al.[21]

Transwell Migration Assay

Serum-starved U937 cells (1×10^6) were placed in 24-well Transwell inserts with 8-μm pores (Corning Life Sciences, Lowell, MA). Cells were allowed to migrate for 2 hours at 37°C toward colon supernatants derived from DSS-induced mice treated with or without YO-2 in the presence of IgG and CXCL5 Ab, or RPMI-1640 medium alone. The number of migrated cells was counted.

Statistical Analyses

All data are presented as means ± SEM. Student *t* tests were performed. Survival curves were plotted using Kaplan–Meier estimates with log rank. A *P* value less than .05 was considered significant.

Results

Plasmin Is Activated During the Early Phase of Experimental Colitis

We investigated whether fibrinolytic factors are present during the progression of IBD by using DSS-induced colitis as a model. An increase in PAP, a measure of active plasmin, was detected in plasma of treated mice, peaking 3 days after the onset of DSS treatment as determined by enzyme-linked immunosorbent assay (Figure 1*A*). We next evaluated the effects of the plasmin inhibitor YO-2 administration on fibrinolytic and coagulation factors. YO-2 blocks the catalytic site of plasmin, and thereby efficiently inhibits active circulating plasmin.[22] YO-2 treatment inhibited the systemic increase in PAP in plasma within the colon of DSS-treated animals (Figure 1*A*). Clinically, IBD patients often show both excessive fibrinolysis and coagulation.[23] Because the function of plasmin is to dissolve fibrin clots, plasmin inhibition might alter coagulation and fibrin deposition/clot formation. However, YO-2 prevented the increase in the coagulation marker thrombin–antithrombin on day 7 (Supplementary Figure 1). Bleeding time was impaired in both phosphate-buffered saline– and YO-2–treated colitic mice (Supplementary Figure 2). No fibrin(ogen) staining pattern was observed in colitic tissues with or without YO-2 on day 7 and YO-2–treated normal colon tissues for 28 days (Supplementary Figure 3). When plasmin breaks down fibrin, FDPs are produced. No significant change in plasma FDP levels was observed in blood samples of DSS-induced colitic mice treated with or without YO-2 (Supplementary Figure 4). The data indicated that a plasmin increase occurs during the early phase of colitis, but no signs of fibrin deposition were found.

Pharmacologic Targeting of Plasmin Prevents DSS-Induced Colitis Progression

Plasmin inhibition by YO-2 treatment protected against DSS-induced colitis-associated lethality, and ameliorated the high DAI (a numeric value reflecting weight loss, diarrhea, and bleeding), and prevented shortening of the colon (Figure 1*B–D*). In line with these observations, colon sections of YO-2–treated mice showed less severe mucosal damage, loss of goblet cells, and inflammatory cell infiltration (Figure 1*E*), indicating that plasmin activation contributes to colitis progression.

Plasmin Regulates uPA-expressing Myeloid Cell Influx Into Colonic Tissues

Plasmin inhibition prevented the recruitment of Gr-1$^+$ CD11b$^+$ neutrophils and F4/80$^+$ CD11b$^+$ macrophages into the mucosal region of the colon (Figure 2*A*). *Plau*

Figure 5. Plasmin inhibition ameliorates TNBS- and CD40-induced colitis. Colitic mice induced by TNBS administration (*left*) or by CD40 Ab injection into *Rag2*$^{-/-}$ mice (*right*) were treated with phosphate-buffered saline (PBS) and YO-2. Levels of PAP in (*A*) plasma and (*B*) TNF-α in serum and in colon supernatants of indicated experimental groups by enzyme-linked immunosorbent assay. (*C*) Body weight loss, with starting body weight set as 100% in control and TNBS- and CD40-treated mice. n = 10/group. (*D*) Representative images of colon sections from TNBS-induced colitic mice stained with H&E, and immunostained using Gr-1, MMP9, and F4/80 Abs. *Scale bars*: 200 μm. (*E*) Representative images of colon sections from CD40 Ab-induced colitic mice stained with H&E, and immunostained using Gr-1, CD11b, and F4/80 Abs. *Scale bars*: 100 μm. YO-2 prevents the infiltration of Gr-1$^+$ neutrophils and F4/80$^+$ macrophages (*white arrows*). (*F*) Quantification of indicated cell populations in indicated treatment groups, n = 3. Data represent means ± SEM. **P* < .05, ***P* < .01, and ****P* < .001, determined by a 2-tailed Student *t* test. HPF, high-power field.

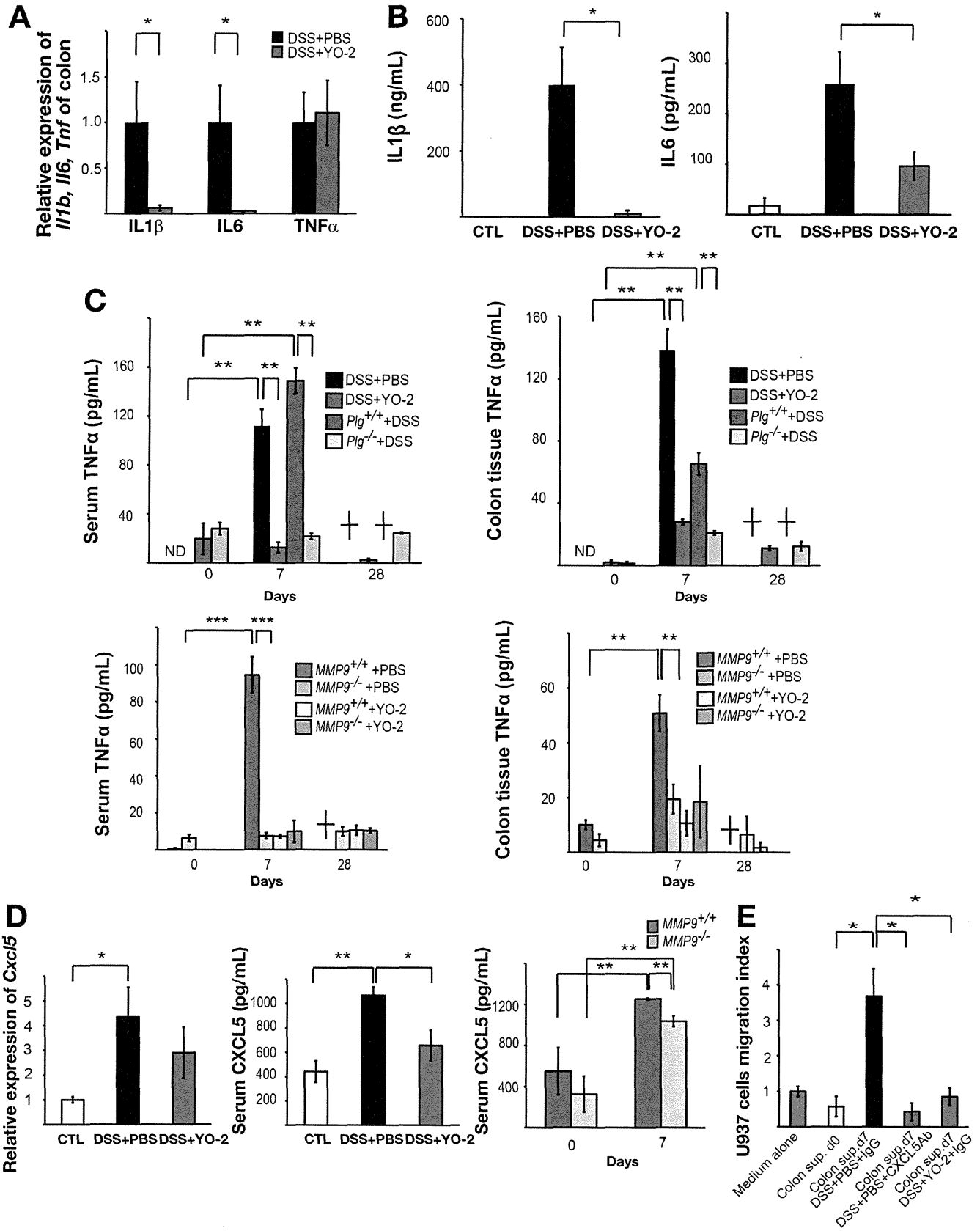
A
Relative expression of Il1b, Il6, Tnf of colon
DSS+PBS
DSS+YO-2
IL1β
IL6
TNFα
B
IL1β (ng/mL)
IL6 (pg/mL)
CTL
DSS+PBS
DSS+YO-2
C
Serum TNFα (pg/mL)
Colon tissue TNFα (pg/mL)
DSS+PBS
DSS+YO-2
Plg+/++DSS
Plg-/-+DSS
ND
Days
MMP9+/+ +PBS
MMP9-/- +PBS
MMP9+/++YO-2
MMP9-/- +YO-2
D
Relative expression of Cxcl5
Serum CXCL5 (pg/mL)
E
U937 cells migration index
Medium alone
Colon sup. d0
Colon sup.d7 DSS+PBS+IgG
Colon sup.d7 DSS+PBS+CXCL5Ab
Colon sup.d7 DSS+YO-2+IgG

(Figure 2*B*), but not *Plat* (data not shown), expression was up-regulated in colon tissues of DSS-treated mice. In accordance with previous studies,[24] YO-2 treatment prevented the influx of uPA–co-expressing $CD11b^+$ cells in colonic tissues (Figure 2*C*). These data suggest that local myelomonocytic cells are a source of uPA during colon inflammation.

Reduced Disease Severity in $Plg^{-/-}$ Mice With DSS-Induced Colitis

To further study the role of Plg in DSS-induced colitis progression, $Plg^{-/-}$ mice were used. $Plg^{-/-}$ mice were protected from DSS-induced colitis, showing a lower mortality rate (Figure 3*A*), a lower DAI (Figure 3*B*), and diminished colon length shortening (Figure 3*B* and *C*). Because colon shortening might be owing to increased cell apoptosis, terminal deoxynucleotidyl transferase–mediated deoxyuridine triphosphate nick-end labeling staining on colon sections was used to determine apoptosis. Fewer terminal deoxynucleotidyl transferase–mediated deoxyuridine triphosphate nick-end labeling–positive cells were observed in $Plg^{-/-}$ mice, indicating that *Plg* deficiency protects from apoptosis in colitic mice (Supplementary Figure 5). $Plg^{-/-}$ mice showed reduced histologic signs of inflammation (Figure 3*D*). Less deposition of collagen and elastic fiber as stained by Elastica van Gieson was observed in $Plg^{-/-}$ colon sections compared with $Plg^{+/+}$ mice (Supplementary Figure 6). These results suggest that plasmin accelerates intestinal inflammation, which might result in increased intestinal apoptosis leading to fibrosis, and, ultimately, causing colon shortening.

Plasmin Enhances Colitis Progression in a Partly MMP9-Dependent Manner

Because plasmin can activate MMPs, and MMPs such as MMP3, MMP7, and MMP12 are linked to the progression of colitis,[25] we hypothesized that plasmin, by activating proteases such as MMP9, might contribute to colitis progression in vivo. Immunoreactive MMP9 was observed in epithelial cells and neutrophils of colon sections derived from DSS-induced colitic mice, but not in YO-2–treated mice (Figure 4*A*). Similarly, YO-2 treatment prevented the increase in total serum MMP9 in YO-2–treated DSS-induced colitic mice (Supplementary Figure 7), with a decrease in both the pro-MMP and active form of MMP9, but not MMP2, as determined by zymography (Figure 4*B*). Similarly, colon supernatants of YO-2–treated DSS-induced colitic mice contained less total MMP9 (Figure 4*C*). DSS-induced colitic $Mmp9^{-/-}$ mice showed an improved survival rate, a lower DAI, prevented infiltration of inflammatory cells, and colonic tissue destruction (Figure 4*D–F*). In comparison with deletion of MMP9 alone, the broad-spectrum MMP inhibitor MMI270, which inhibits several MMPs, ameliorated colitis progression to a greater extent (Figure 4*D*). However, when comparing YO-2– and MMI270-treated mice, YO-2–treated mice showed the best survival rate because 10% of MMI270-treated mice died after suffering from a musculoskeletal syndrome, a known side effect of MMP inhibitors containing a hydroxamate structure.[26] No side effects were observed in YO-2–treated mice.

Plasmin Inhibition Ameliorates Colitis After TNBS and CD40 Induction

We extended our analysis by evaluating the effect of plasmin inhibition in 2 other colitis models: the TNBS-induced colitis model and the anti-CD40 colitis model. In YO-2–treated colitic mice, no increase in circulating plasmin level and no augmentation in colon-derived or circulating TNF-α level was observed (Figure 5*A* and *B*). YO-2 treatment prevented colitis-related body weight loss (Figure 5*C*) and the destruction of the colonic epithelium in both colitis models (Figure 5*D* and *E*). Immunoreactive MMP9 was found in the colonic tissue of phosphate-buffered saline–treated, but not YO-2–treated, mice in TNBS colitis (Figure 5*D*). In addition, YO-2 treatment reduced the number of infiltrating inflammatory $Gr\text{-}1^+$ and $F4/80^+$ myeloid cells (Figure 5*F*). These data suggest that plasmin inhibition suppressed clinical progression of the colitis-associated cytokine storm in 3 murine models of colitis.

Figure 6. Pharmacologic plasmin inhibition alleviates systemic and colonic cytokine production in DSS-induced colitic mice. (*A*) Gene expression of *Il1b*, *Il6*, and *Tnf* in colon homogenates of C57BL/6 mice treated with phosphate-buffered saline (PBS) or YO-2 as determined by polymerase chain reaction (normalized to the expression of *Actb*). n = 4 or 5/group. (*B*) The inflammatory cytokines IL1β and IL6 were assayed in serum samples of mice with DSS-induced colitis treated with or without YO-2 as determined by enzyme-linked immunosorbent assay. n = 6/group. (*C*) TNF-α levels were measured in serum samples (*left panel*) or in supernatants (*right panel*) of cultured colon tissue retrieved from YO-2– or PBS-treated C57BL/6 mice, $Plg^{+/+}$ or $Plg^{-/-}$, and $Mmp9^{+/+}$ and $Mmp9^{-/-}$ mice 7 days after the initiation of DSS treatment by enzyme-linked immunosorbent assay. n = 3–6/group. (*D*) *CXCL5* expression in colon samples extracted from DSS-induced colitic mice treated with or without YO-2 (*left panel*). CXCL5 levels in serum of YO-2– or PBS-treated C57BL/6 mice (*middle panel*) and $Mmp9^{-/-}$ (*right panel*), or their respective littermate controls as determined by enzyme-linked immunosorbent assay. n = 3–6/group. (*E*) Transmigration index of U937 cells migrating toward medium alone, colon supernatants extracted from normal mice (d0), or supernatants from DSS-treated mice injected with PBS or YO-2 in the presence or absence of CXCR5 Ab. n = 3–5/group. Data represent means ± SEM. $^*P < .05$ and $^{**}P < .01$, determined by a 2-tailed Student *t* test. CTL, control day 0.

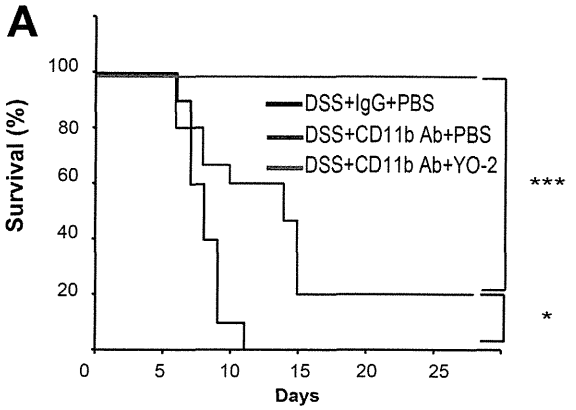
A
Survival (%)
100
80
60
40
20
0
5
10
15
20
25
Days
DSS+IgG+PBS
DSS+CD11b Ab+PBS
DSS+CD11b Ab+YO-2
***
*

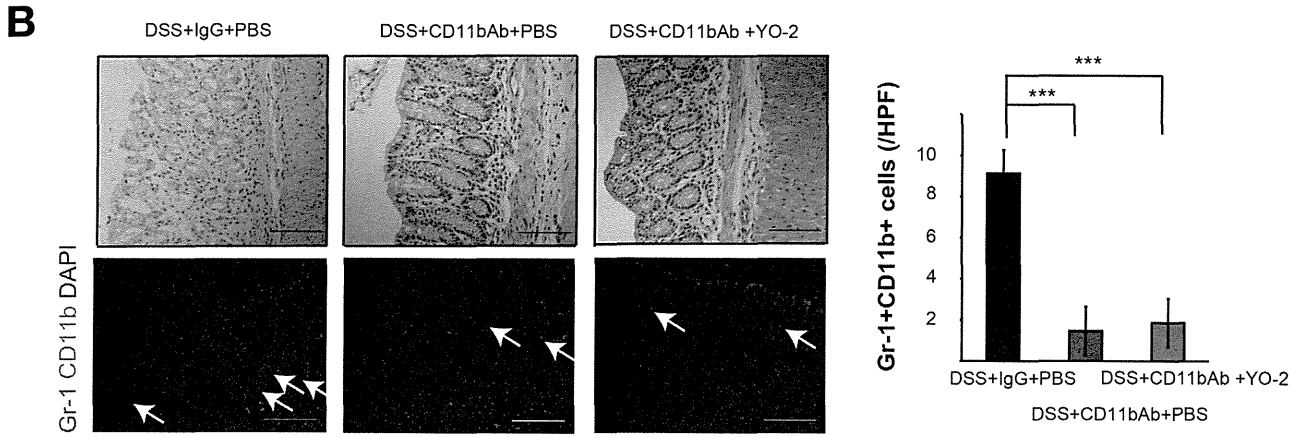
B
DSS+IgG+PBS
DSS+CD11bAb+PBS
DSS+CD11bAb +YO-2
Gr-1 CD11b DAPI
Gr-1+CD11b+ cells (/HPF)
10
8
6
4
2
***
***
DSS+IgG+PBS
DSS+CD11bAb +YO-2
DSS+CD11bAb+PBS

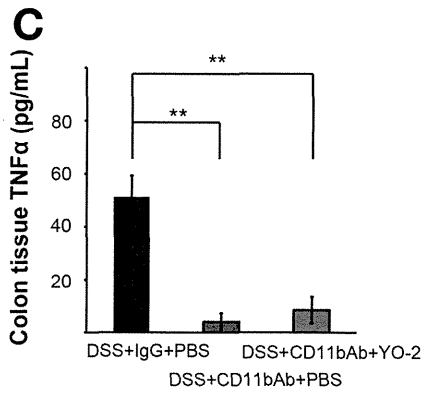
C
Colon tissue TNFα (pg/mL)
80
60
40
20
**
**
DSS+IgG+PBS
DSS+CD11bAb+YO-2
DSS+CD11bAb+PBS

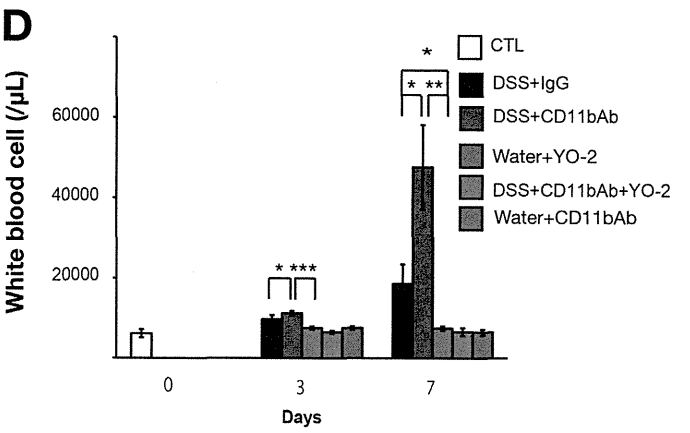
D
White blood cell (/μL)
60000
40000
20000
0
3
7
Days
CTL
DSS+IgG
DSS+CD11bAb
Water+YO-2
DSS+CD11bAb+YO-2
Water+CD11bAb
*
* **
* ***

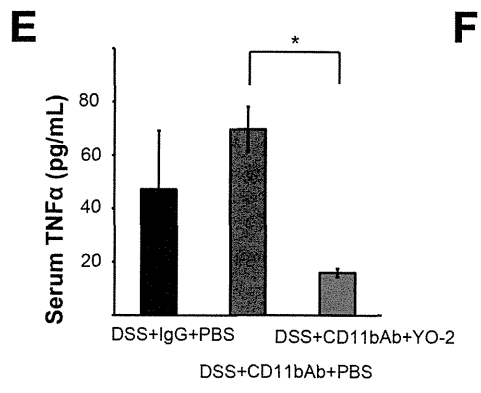
E
Serum TNFα (pg/mL)
80
60
40
20
*
DSS+IgG+PBS
DSS+CD11bAb+YO-2
DSS+CD11bAb+PBS

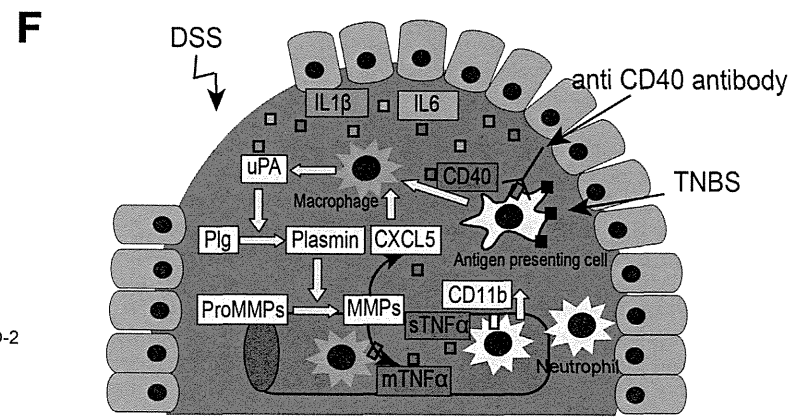
F
DSS
anti CD40 antibody
TNBS
IL1β
IL6
uPA
CD40
Macrophage
Plg
Plasmin
CXCL5
Antigen presenting cell
ProMMPs
MMPs
CD11b
sTNFα
mTNFα
Neutrophil

Plasmin and Mmp9 Deficiency Reduce the Cytokine Storm Associated With Colitis

We next examined typical IBD-associated cytokines in DSS-induced colitis. The expression of *Il1b* and *Il6* messenger RNA (Figure 6*A*) in colonic extracts and circulating IL1β and IL6 (Figure 6*B*) was lower in YO-2–treated colitic mice. Plasmin deletion or inhibition and *Mmp9* deficiency prevented the increase in circulating TNF-α serum levels and suppressed TNF-α release from colonic supernatants after DSS induction (Figure 6*A–C*). Although MMP9 is a downstream target of plasmin, plasma PAP levels were low in colitic *Mmp9*$^{-/-}$ mice (Supplementary Figure 8) by preserving (eg, crypt destruction and epithelial cell sloughing). These data indicate that plasmin is important in mounting a cytokine response.

Reduced CXCL5 Release During Colitis After Plasmin and MMP9 Inhibition

In vivo processing of CXCL5 by MMP2 and MMP9 promotes neutrophil recruitment in a model of peritonitis.[27] Although YO-2 treatment did not alter *Cxcl5* gene expression significantly, in YO-2–treated mice and *MMP9*$^{-/-}$ mice no increase in serum CXCL5 levels was observed (Figure 6*D*). We investigated whether CXCL5 is released from colonic tissues and might be involved in leukocyte migration. The improved myeloid (U937) cell migration toward supernatants derived from colitic mice was the result of plasmin/MMP9-dependent production of CXCL5, as shown using neutralizing Abs (Figure 6*E*). These data show that plasmin enhances the colon-derived release of CXCL5, thereby enhancing neutrophil influx.

CD11b$^+$ Cells Drive Plasmin-Mediated Colitis Progression

If the recruitment of CD11b$^+$ cells is the main function of plasmin-mediated effects during colitis, blocking CD11b cell recruitment using CD11b neutralizing Abs should improve clinical signs of colitis. However, this was not the case (Figure 7*A*). Similar to previous reports,[28] 80% of DSS-induced mice treated with neutralizing Abs against CD11b died (Figure 7*A*), although CD11b$^+$ cell influx into colonic tissues (Figure 7*B*) and local colonic TNF-α production was blocked (Figure 7*C*). Mononuclear cells isolated from the blood of CD11b Ab-treated, but not YO-2–treated, mice showed high *Tnf* messenger RNA expression (Supplementary Figure 9). A systemic TNF-α increase correlated with leukocytosis by mononuclear cells, whereas local colonic TNF-α production correlated with the number of infiltrated CD11b$^+$ cells (Figure 7*C–E*). Survival, white blood cell counts, histopathologic changes, and TNF-α serum level increase were suppressed after co-injection of YO-2 with CD11b Abs (Figure 7*A–E*). Our data suggest that plasmin promotes colitis progression by accelerating leukocytosis and leukocyte activation, resulting in the release of TNF-α, and by enhancing the infiltration of myeloid cells into colonic tissues.

Taken together, our data indicate that the activation of the fibrinolytic pathway accelerates the inflammatory response during colitis progression by the influx of CD11b$^+$ myeloid cells.

Discussion

In this study, we provide genetic, functional, and biochemical evidence that the orderly activation of 2 separate protease systems, the fibrinolytic system and the MMP system during experimental colitis, drives mucosal inflammation, a process in part mediated by an accelerating systemic and colonic increase in CD11b$^+$ inflammatory cells and the release of the proinflammatory cytokine TNF-α and of the chemokine CXCL5. Collectively, these data introduce a novel paradigm by which fibrinolytic enzymes mediate systemic and localized effects in the colonic tissues and establish a novel role for Plg activation in colitis. We recently showed that addition of TNF-α to myeloid cells increased the expression of uPA in vitro.[29] We found local up-regulation of the uPA in inflamed, but not control, colonic tissues. The observed low uPA expression in colitic tissues in plasmin inhibitor-treated mice could be owing to the impaired infiltration of uPA-producing CD11b$^+$ cells and/or

Figure 7. Improved disease control and inflammatory cytokine response in YO-2–treated compared with CD11b Ab–treated mice during experimental colitis. DSS-induced C57BL/6 mice were treated with YO-2 and co-injected with anti-CD11b or control Abs. (*A*) The survival rate was determined in the following treatment groups: 2% DSS + IgG + phosphate-buffered saline (PBS), n = 10; 2% DSS + CD11b Ab + PBS, n = 15; 2% DSS + CD11b Ab + YO-2, n = 10. (*B*) Representative H&E-stained colon sections from treated mice. *Scale bars*: 200 μm. (*C*) TNF-α protein in supernatants from colon cultures at day 7. (*D*) White blood cells were counted at the indicated time points. n = 6/group. (*E*) TNF-α protein was determined in plasma samples taken at day 7. Dates represent means ± SEM. *$P < .05$, **$P < .01$, and ***$P < .001$, determined by a 2-tailed Student *t* test and log-rank test. (*F*) A model of various target molecules of plasmin involved in experimentally induced colitis. The secreted plg is processed into its enzymatically active form plasmin by uPA, which is supplied by the activated CD11b$^+$ inflammatory cells during colitis. Plasmin in turn sensitizes macrophages and/or epithelium to accelerate the conversion from pro-MMP9 to MMP9. The proteolytic environment generated not only damage to colonic tissues, but also releases proinflammatory cytokines (eg, TNF-α) and chemokines (eg, CXCL5) known to promote the influx of CD11b$^+$ cells into colonic tissues. These CD11b$^+$ cells promote colonic tissue damage in part by again providing necessary proteases to fuel this vicious cycle. DAPI, 4′,6-diamidino-2-phenylindole.

the blockade of local and systemic TNF-α increase. Our data showing the PAP increase in DSS-treated mice are in accordance with clinical reports from patients with IBD.[30] The presence of fibrinolytic factors within colonic tissues (eg, uPA-expressing myeloid cells),[24] suggest that localized proteolysis occurs during colitis, paving the way for inflammatory cells or intestinal microbes to further induce tissue damage. Our data are shown in Figure 7*F*.

The fibrinolytic system is activated in IBD patients; this is especially true for patients with active disease.[31,32] Our initial decision to explore the therapeutic potential of YO-2 was motivated by previous studies showing that administration of the antifibrinolytic agents ε-aminocaproic acid and tranexamic acid improved clinical outcomes of patients with UC.[33,34] Here, we show that plasmin inhibition enabled recovery from colitis-induced tissue damage and improved clinical outcomes.

What are the potential downstream targets of plasmin during the colitis process? We were able to show that the activation of MMPs such as MMP9 is a critical downstream event during colitis progression. Plasmin has been shown to activate MMP9 in other disease models, including nerve injury,[28] disease progression in acute graft-versus-host disease after bone marrow transplantation,[29] and hematopoietic and ischemic tissue regeneration.[7,9] It has been well established that MMP9 is up-regulated consistently in both animal models and human IBD, and is associated with disease severity.[3,35] Confirming data by Castaneda et al,[3] we showed that *MMP9*$^{-/-}$ mice exposed to DSS showed reduced colitis severity. Epithelial MMP9 but not infiltrated neutrophil-derived MMP9, has been shown to induce tissue damage. Here, we found that plasmin inhibition prevented MMP9 activation and TNF-α release both systemically and locally in the colonic environment. TNF-α release involves a process called shedding, which involves the protease ADAM17/TNF-α converting enzyme, but also other MMPs such as MMP1, MMP7, and MMP9.[36] Our data indicate that plasmin-dependent TNF-α production requires endogenous MMP9, which promotes TNF-α production either directly or indirectly by activating other proteases. However, YO-2 also seems to have MMP9-independent modes of action because YO-2 treatment improved survival even in *Mmp9*$^{-/-}$ mice. Because plasmin can activate other MMPs such as MMP3, MMP7, and MMP12, which are linked to the progression of colitis,[25] we suspect that the control of other MMPs might be responsible for the improved survival of *Mmp9*$^{-/-}$ mice treated with YO-2.

Anti-inflammatory medication is a mainstay of IBD treatment. Infliximab, a monoclonal Ab to TNF-α, appeared to be a good therapeutic agent for IBD patients.[37] However, aside from its high expense, Ab treatment can lead to infusion reactions, loss of response, and serum sickness.[38] Use of small molecules such as the plasmin inhibitor not only would be cheaper, but might even be safer because there is less risk of immunogenicity in patients. Furthermore, YO-2 could prevent the other inflammatory cytokines IL1β and IL6.

The influx of CD11b^{+} macrophages and neutrophils into the inflamed tissue is a critical pathogenic aspect of colitis in a plasmin-dependent manner. CD11b interacts with the intercellular adhesion molecules intercellular adhesion molecules 1 and 2,[39] which have been suggested as therapeutic targets in colitis. Although CD11b Ab treatment slightly improved survival in colitic mice, the Abs could not control systemic TNF-α release, so that peripheral leukocytosis proceeded unabated. These data are consistent with that of other inflammatory models, such as peritonitis, in which CD11b Ab treatment prevented myelomonocytic cell recruitment in vivo.[40]

We previously showed that plasmin regulates Gr-1^{+} neutrophil infiltration during recovery from hindlimb ischemia.[8] Here, we found that plasmin inhibition prevented the infiltration of Gr-1^{+} neutrophils into colonic tissues. Enterocyte-derived CXCL5 can attract CXCR2+ neutrophils into the gut tissues.[41] Recently, it was shown that in vivo processing of CXCL5, MMP2, and MMP9 promotes neutrophil recruitment in IL1β-induced peritonitis.[27] Circulating CXCL5 was suppressed both in YO-2–treated mice and in *MMP9*$^{-/-}$ mice, showing that YO-2 (most likely via MMP inhibition, however, further studies are necessary) can control CXCL5 production, thereby preventing influx of MMP9-carrying neutrophils.

Our data support a mechanism whereby activation of Plg during colitis progression leads to the activation of another protease cascade, namely MMPs. This proteolytic environment controls both cell infiltration into colonic tissues, as well as production and secretion of proinflammatory cytokines and chemokines. In contrast to TNF-α Abs, the targeting of plasmin can suppress the MMP cascade, thereby controlling the release of important proinflammatory cytokines. Our experimental approach here was prophylactic, but our findings suggest that YO-2 is an attractive candidate for targeting milder forms of IBD after onset.

Supplementary Material

Note: To access the supplementary material accompanying this article, visit the online version of *Gastroenterology* at www.gastrojournal.org, and at http://dx.doi.org/10.1053/j.gastro.2014.12.001.

References

1. Podolsky DK. Inflammatory bowel disease. N Engl J Med 2002;347:417–429.
2. Heissig B, Nishida C, Tashiro Y, et al. Role of neutrophil-derived matrix metalloproteinase-9 in tissue regeneration. Histol Histopathol 2010;25:765–770.
3. Castaneda FE, Walia B, Vijay-Kumar M, et al. Targeted deletion of metalloproteinase 9 attenuates experimental

colitis in mice: central role of epithelial-derived MMP. Gastroenterology 2005;129:1991–2008.
4. Mao JW, He XM, Tang HY, et al. Protective role of metalloproteinase inhibitor (AE-941) on ulcerative colitis in rats. World J Gastroenterol 2012;18:7063–7069.
5. Lijnen HR, Silence J, Lemmens G, et al. Regulation of gelatinase activity in mice with targeted inactivation of components of the plasminogen/plasmin system. Thromb Haemost 1998;79:1171–1176.
6. Heissig B, Ohki-Koizumi M, Tashiro Y, et al. New functions of the fibrinolytic system in bone marrow cell-derived angiogenesis. Int J Hematol 2012;95:131–137.
7. **Ohki M, Ohki Y**, Ishihara M, et al. Tissue type plasminogen activator regulates myeloid-cell dependent neoangiogenesis during tissue regeneration. Blood 2010; 115:4302–4312.
8. Tashiro Y, Nishida C, Sato-Kusubata K, et al. Inhibition of PAI-1 induces neutrophil-driven neoangiogenesis and promotes tissue regeneration via production of angiocrine factors in mice. Blood 2012;119:6382–6393.
9. Heissig B, Lund LR, Akiyama H, et al. The plasminogen fibrinolytic pathway is required for hematopoietic regeneration. Cell Stem Cell 2007;1:658–670.
10. Black RA, Rauch CT, Kozlosky CJ, et al. A metalloproteinase disintegrin that releases tumour-necrosis factor-alpha from cells. Nature 1997;385: 729–733.
11. Hattori K, Hirano T, Ushiyama C, et al. A metalloproteinase inhibitor prevents lethal acute graft-versus-host disease in mice. Blood 1997;90:542–548.
12. Neurath MF, Fuss I, Pasparakis M, et al. Predominant pathogenic role of tumor necrosis factor in experimental colitis in mice. Eur J Immunol 1997;27:1743–1750.
13. Doe WF, Dorsman B. Chronic inflammatory bowel disease–increased plasminogen activator secretion by mononuclear phagocytes. Clin Exp Immunol 1982; 48:256–260.
14. Souto JC, Martinez E, Roca M, et al. Low levels of plasminogen activator inhibitor type 1 in patients with inflammatory bowel disease. Fibrinolysis 1994;8: 359–363.
15. **Uhlig HH, McKenzie BS**, Hue S, et al. Differential activity of IL-12 and IL-23 in mucosal and systemic innate immune pathology. Immunity 2006;25:309–318.
16. Cayatte C, Joyce-Shaikh B, Vega F, et al. Biomarkers of therapeutic response in the IL-23 pathway in inflammatory bowel disease. Clin Transl Gastroenterol 2012;3:e10.
17. Okada Y, Tsuda Y, Tada M, et al. Development of potent and selective plasmin and plasma kallikrein inhibitors and studies on the structure-activity relationship. Chem Pharm Bull (Tokyo) 2000;48:1964–1972.
18. Peterson JT. Matrix metalloproteinase inhibitor development and the remodeling of drug discovery. Heart Fail Rev 2004;9:63–79.
19. Cooper HS, Murthy SN, Shah RS, et al. Clinicopathologic study of dextran sulfate sodium experimental murine colitis. Lab Invest 1993;69:238–249.
20. Wirtz S, Neufert C, Weigmann B, et al. Chemically induced mouse models of intestinal inflammation. Nat Protocols 2007;2:541–546.
21. **Heissig B, Hattori K**, Dias S, et al. Recruitment of stem and progenitor cells from the bone marrow niche requires MMP-9 mediated release of kit-ligand. Cell 2002; 109:625–637.
22. Lee E, Enomoto R, Takemura K, et al. A selective plasmin inhibitor, trans-aminomethylcyclohexanecarbonyl-L-(O-picolyl)tyrosine-octylamide (YO-2), induces thymocyte apoptosis. Biochem Pharmacol 2002;63:1315–1323.
23. van Bodegraven AA, Schoorl M, Linskens RK, et al. Persistent activation of coagulation and fibrinolysis after treatment of active ulcerative colitis. Eur J Gastroenterol Hepatol 2002;14:413–418.
24. Vassalli JD, Dayer JM, Wohlwend A, et al. Concomitant secretion of prourokinase and of a plasminogen activator-specific inhibitor by cultured human monocytes-macrophages. J Exp Med 1984;159:1653–1668.
25. Naito Y, Takagi T, Kuroda M, et al. An orally active matrix metalloproteinase inhibitor, ONO-4817, reduces dextran sulfate sodium-induced colitis in mice. Inflamm Res 2004;53:462–468.
26. Fisher JF, Mobashery S. Recent advances in MMP inhibitor design. Cancer Metastasis Rev 2006;25: 115–136.
27. Song J, Wu C, Zhang X, et al. In vivo processing of CXCL5 (LIX) by matrix metalloproteinase (MMP)-2 and MMP-9 promotes early neutrophil recruitment in IL-1beta-induced peritonitis. J Immunol 2013;190: 401–410.
28. Zou T, Ling C, Xiao Y, et al. Exogenous tissue plasminogen activator enhances peripheral nerve regeneration and functional recovery after injury in mice. J Neuropathol Exp Neurol 2006;65:78–86.
29. Vrij AA, Rijken J, van Wersch JW, et al. Coagulation and fibrinolysis in inflammatory bowel disease and in giant cell arteritis. Pathophysiol Haemost Thromb 2003;33: 75–83.
30. Koutroubakis IE. Therapy insight: vascular complications in patients with inflammatory bowel disease. Nat Clin Pract Gastroenterol Hepatol 2005;2:266–272.
31. Kume K, Yamasaki M, Tashiro M, et al. Activations of coagulation and fibrinolysis secondary to bowel inflammation in patients with ulcerative colitis. Intern Med 2007;46:1323–1329.
32. Salter RH, Read AE. Epsilon-aminocaproic acid therapy in ulcerative colitis. Gut 1970;11:585–587.
33. Hollanders D, Thomson JM, Schofield PF. Tranexamic acid therapy in ulcerative colitis. Postgrad Med J 1982; 58:87–91.
34. Sato A, Nishida C, Sato-Kusubata K, et al. Inhibition of plasmin attenuates murine acute graft-versus-host disease mortality by suppressing the matrix metalloproteinase-9-dependent inflammatory cytokine storm and effector cell trafficking. Leukemia 2015; 29:145–156.
35. Kolho KL, Sipponen T, Valtonen E, et al. Fecal calprotectin, MMP-9, and human beta-defensin-2 levels in pediatric inflammatory bowel disease. Int J Colorectal Dis 2014;29:43–50.
36. Mohan MJ, Seaton T, Mitchell J, et al. The tumor necrosis factor-alpha converting enzyme (TACE): a unique

metalloproteinase with highly defined substrate selectivity. Biochemistry 2002;41:9462–9469.
37. Jarnerot G, Hertervig E, Friis-Liby I, et al. Infliximab as rescue therapy in severe to moderately severe ulcerative colitis: a randomized, placebo-controlled study. Gastroenterology 2005;128:1805–1811.
38. Rutgeerts P, Van Assche G, Vermeire S. Optimizing anti-TNF treatment in inflammatory bowel disease. Gastroenterology 2004;126:1593–1610.
39. Sans M, Panes J, Ardite E, et al. VCAM-1 and ICAM-1 mediate leukocyte-endothelial cell adhesion in rat experimental colitis. Gastroenterology 1999;116:874–883.
40. Rosen H, Gordon S. Monoclonal antibody to the murine type 3 complement receptor inhibits adhesion of myelomonocytic cells in vitro and inflammatory cell recruitment in vivo. J Exp Med 1987;166:1685–1701.
41. Mei J, Liu Y, Dai N, et al. Cxcr2 and Cxcl5 regulate the IL-17/G-CSF axis and neutrophil homeostasis in mice. J Clin Invest 2012;122:974–986.

Author names in bold designate shared co-first authorship.

Received January 14, 2014. Accepted December 2, 2014.

Reprint requests
Address requests for reprints to: Koichi Hattori, MD, PhD, Center for Stem Cell Biology and Regenerative Medicine, Institute of Medical Science, University of Tokyo, 4-6-1, Shirokanedai, Minato-ku, Tokyo 108-8639, Japan. e-mail: khattori@ims.u-tokyo.ac.jp; fax: (81) 3-5449-5742.

Acknowledgments
The authors thank Stephanie C. Napier and Robert Whittier for kindly providing editorial assistance to the authors during the preparation of this manuscript.

Conflicts of interest
The authors disclose no conflicts.

Funding
Supported by grants from the Japan Society for the Promotion of Science and Grants-in-Aid for Scientific Research from the Ministry of Education, Culture, Sports, Science and Technology (K.H.,B.H.,Y.T.); Grant-in-Aid for Scientific Research on Priority Areas from the Ministry of Education, Culture, Sports, Science and Technology (K.H.); the Mitsubishi Pharma Research Foundation (K.H); Grant-in-Aid for Scientific Research on Innovative Areas from the Ministry of Education, Culture, Sports, Science and Technology (B.H.); and the Program for Improvement of the Research Environment for Young Researchers (B.H.) funded by the Special Coordination Funds for Promoting Science and Technology of the Ministry of Education, Culture, Sports, Science and Technology.

Supplementary Material

Supplementary Figures 1–9. DSS-induced mice were treated with or without YO-2. Data represent means ± SEM. $*P < .05$, $**P < .01$, and $***P < .001$, determined by a 2-tailed Student t test.

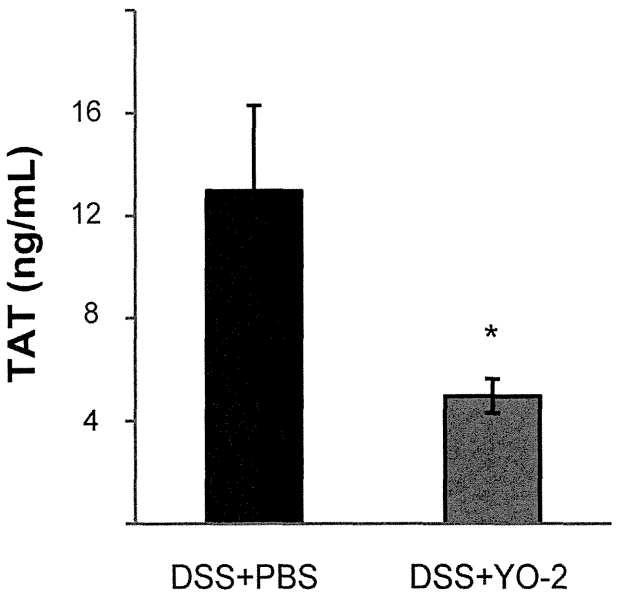

Supplementary Figure 1. The coagulation marker TAT is increased in the plasma of phosphate-buffered saline (PBS)-treated colitic mice, but not YO-2–treated mice, as determined by enzyme-linked immunosorbent assay at day 7. n = 3/group.

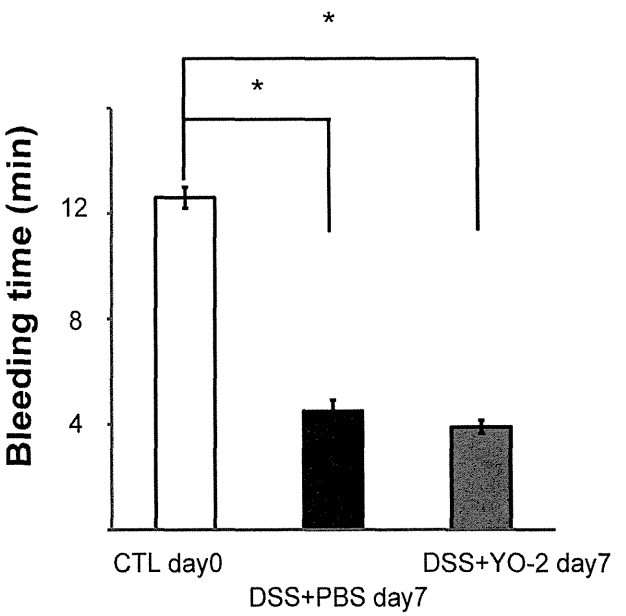

Supplementary Figure 2. Bleeding time was impaired in both phosphate-buffered saline (PBS)- and YO-2–treated DSS-induced mice at day 7. n = 6/group.

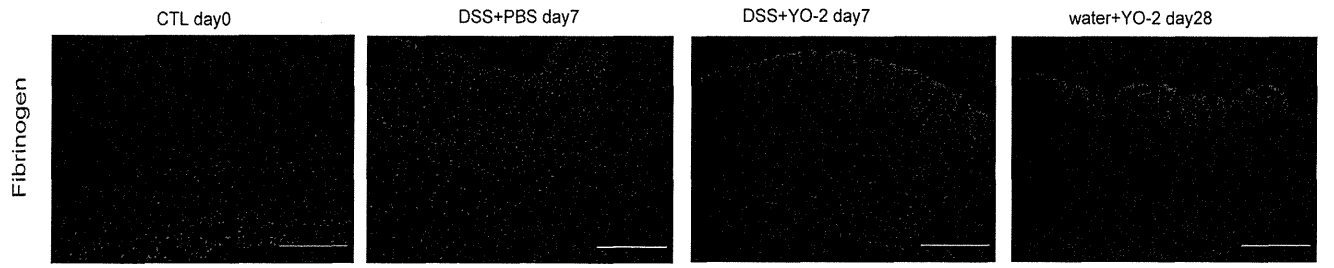

Supplementary Figure 3. Fibrin/fibrinogen immunostaining of colon tissues. No fibrin deposit was detected in colitic tissues after 7 days of DSS ingestion with/without YO-2 and in colon tissues of mice that had been treated for 28 days with YO-2. N = 3/group. CTL, control day 0; PBS, phosphate-buffered saline.

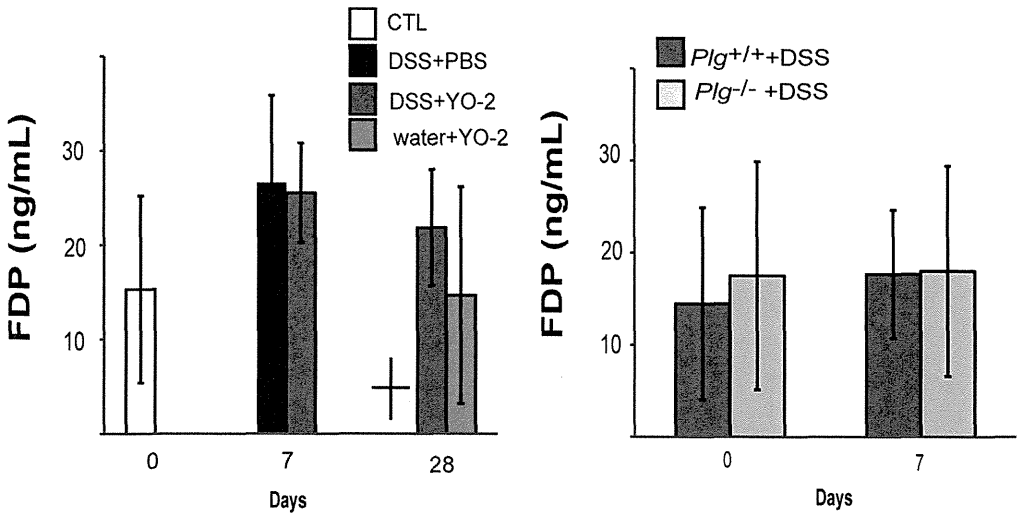

Supplementary Figure 4. FDP levels in blood samples of mice were analyzed. n = 3–6/group. CTL, control day 0; PBS, phosphate-buffered saline.

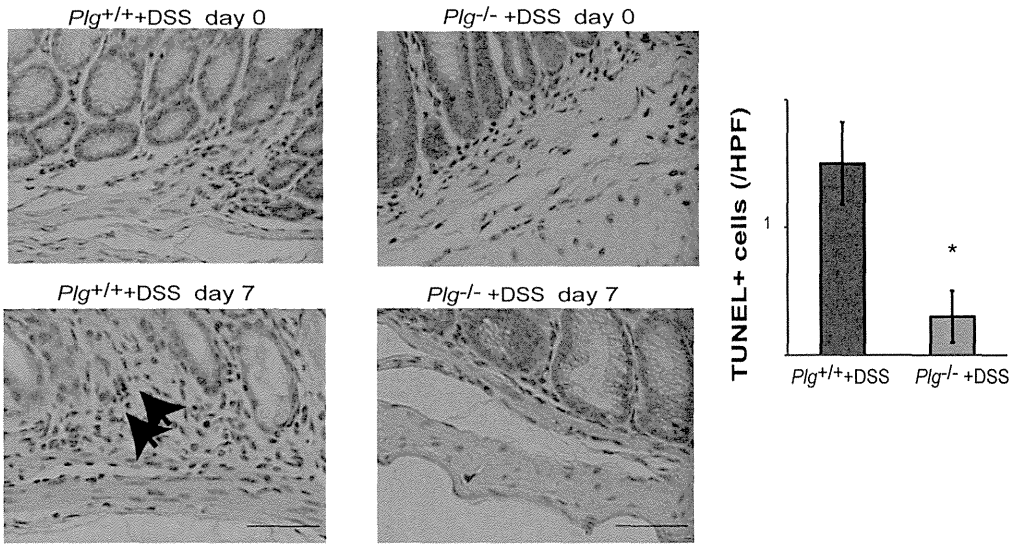

Supplementary Figure 5. Terminal deoxynucleotidyl transferase–mediated deoxyuridine triphosphate nick-end labeling (TUNEL) staining of colon tissues showed an increased number of TUNEL$^+$ cells in the control treated group (*left panel*). *Arrows* indicate TUNEL positively stained cells. $n = 3$/group. *Right*: Quantification of the number of TUNEL$^+$ cells per high-power field (HPF). *Scale bars*: 20 μm.

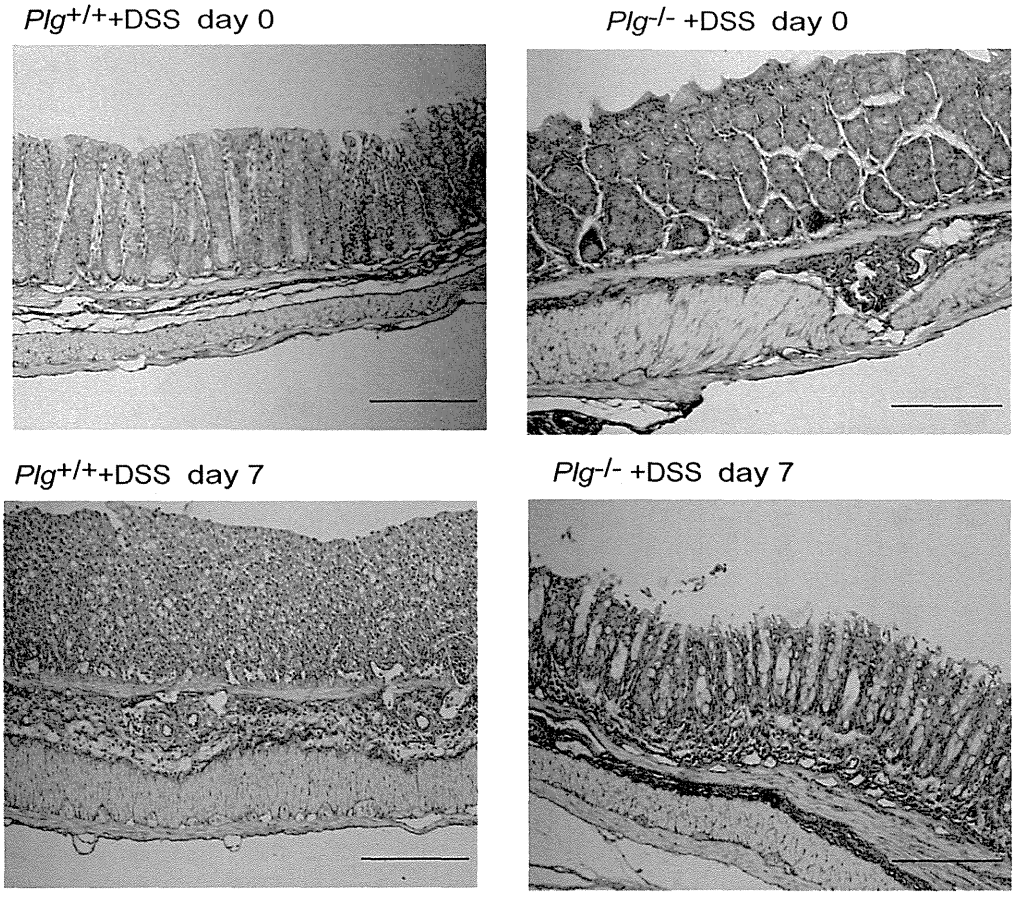

Supplementary Figure 6. Elastica van Gieson staining (blue staining, used to differentiate between collagen and smooth muscle; collagen stains bright red; and cytoplasm, muscle, and fibrin stain yellow) of colon tissues obtained from DSS-treated *Plg*$^{+/+}$ and *Plg*$^{-/-}$ mice. *Scale bars*: 200 μm.

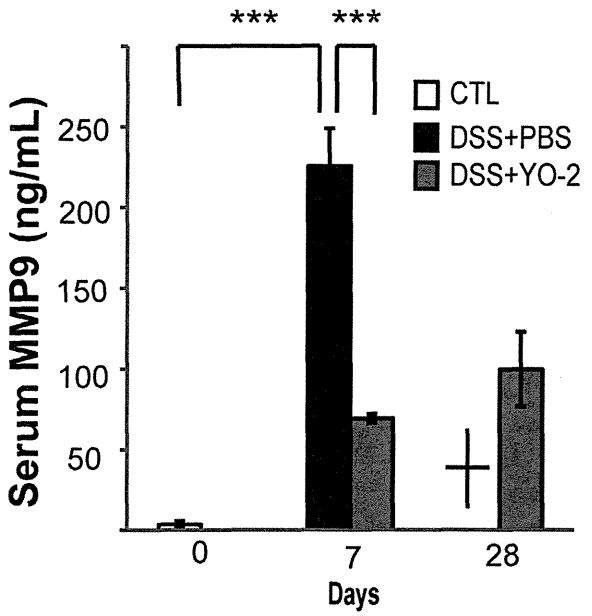

Supplementary Figure 7. MMP9 serum levels assayed in YO-2– or phosphate-buffered saline (PBS)-treated C57BL/6 mice by enzyme-linked immunosorbent assay. $n = 3$/group.

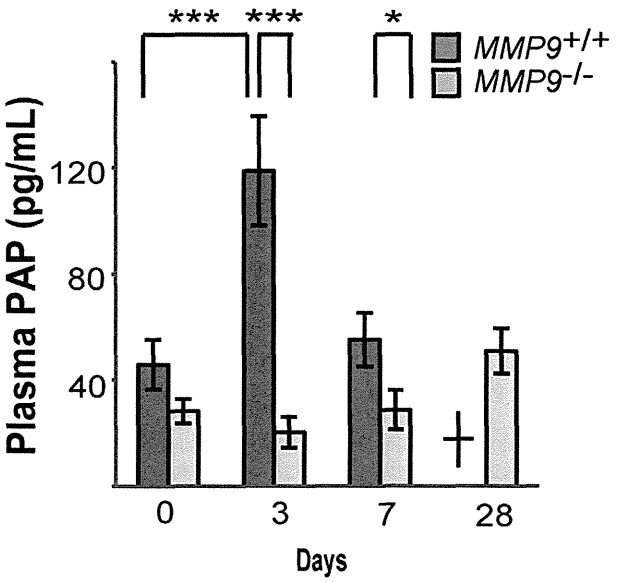

Supplementary Figure 8. PAP plasma levels in DSS-treated *Mmp9*$^{+/+}$ and *Mmp9*$^{-/-}$ mice by enzyme-linked immunosorbent assay. $n = 3$/group.

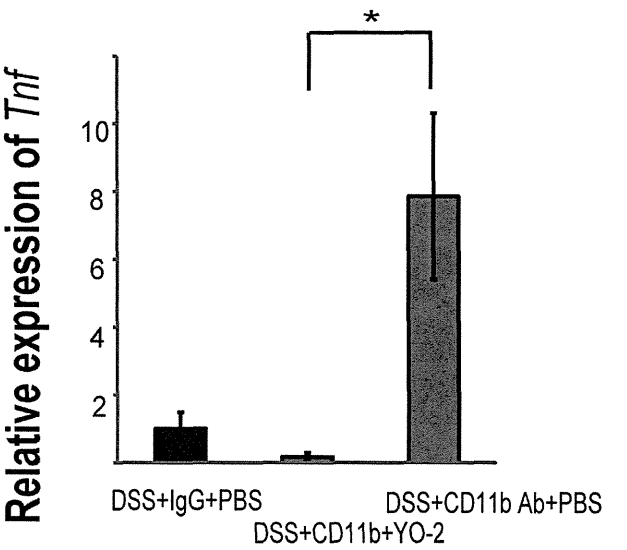

Supplementary Figure 9. *Tnf* expression in circulating mononuclear cells of indicated groups at day 7. $n = 3$/group. PBS, phosphate-buffered saline.

Leukemia (2015) **29,** 145–156
© 2015 Macmillan Publishers Limited All rights reserved 0887-6924/15
www.nature.com/leu

ORIGINAL ARTICLE

Inhibition of plasmin attenuates murine acute graft-versus-host disease mortality by suppressing the matrix metalloproteinase-9-dependent inflammatory cytokine storm and effector cell trafficking

A Sato[1], C Nishida[1,2], K Sato-Kusubata[2], M Ishihara[1], Y Tashiro[1], I Gritli[1], H Shimazu[1], S Munakata[1], H Yagita[3], K Okumura[3], Y Tsuda[4], Y Okada[4], A Tojo[5], H Nakauchi[5], S Takahashi[5], B Heissig[2,3,6] and K Hattori[1,3,6]

The systemic inflammatory response observed during acute graft-versus-host disease (aGVHD) is driven by proinflammatory cytokines, a 'cytokine storm'. The function of plasmin in regulating the inflammatory response is not fully understood, and its role in the development of aGVHD remains unresolved. Here we show that plasmin is activated during the early phase of aGVHD in mice, and its activation correlated with aGVHD severity in humans. Pharmacological plasmin inhibition protected against aGVHD-associated lethality in mice. Mechanistically, plasmin inhibition impaired the infiltration of inflammatory cells, the release of membrane-associated proinflammatory cytokines including tumor necrosis factor-α (TNF-α) and Fas-ligand directly, or indirectly via matrix metalloproteinases (MMPs) and alters monocyte chemoattractant protein-1 (MCP-1) signaling. We propose that plasmin and potentially MMP-9 inhibition offers a novel therapeutic strategy to control the deadly cytokine storm in patients with aGVHD, thereby preventing tissue destruction.

Leukemia (2015) **29,** 145–156; doi:10.1038/leu.2014.151

INTRODUCTION

Allogeneic hematopoietic stem cell transplantation (allo-HSCT) is the only curative option for many hematological malignancies. However, the development of acute graft-versus-host disease (aGVHD) limits the success of allo-HSCT and is fatal in approximately 15% of transplant recipients. In the first phase of aGVHD, antigen-presenting cells are stimulated due to antigen disparities between host and graft.[1,2] Donor T cells are activated, and T-helper 1 (T_H1) cytokines like interferon-γ (IFN-γ), interleukin-2 (IL-2) and tumor necrosis factor-α (TNF-α) initiate the recruitment of effector cells (cytotoxic T lymphocytes, natural killer cells and monocytes). Finally, TNF-α, IL-1 and IFN-γ as inflammatory mediators induce end-organ damage. A network of soluble cytokines, a so-called 'cytokine storm', forms a critical link between each of these steps and may be responsible for the bulk of target-organ damage.[3] The 'cytokine storm' drives the systemic inflammatory response observed in septic shock and aGVHD, accelerates the coagulation/fibrinolytic system and generates an imbalance between coagulation and fibrinolysis.[4,5] Plasmin (plm), a serine protease, is generated by conversion from plasminogen (plg) by two plasminogen activators (PA), such as tissue-type PA (tPA) and urokinase-type PA (uPA). Although tPA has a dominant role in the resolution of fibrin clots (fibrinolysis), uPA can activate extracellular proteolysis during inflammatory processes.[6] Plm/plg binds to cells like monocytes via receptors (annexin 2 and Plg-R_{KT}),[7] can alter the expression of cytokines such as TNF-α, IL-1, IL-6 and monocyte chemoattractant protein-1 (MCP)-1[8–11] and modify cell migration.[12–14] The role of plm in guiding the cytokine storm is not well understood. Because plm can activate other proteases like metalloproteinases (MMPs)[15–17] and some MMP inhibitors can block processing of TNF-α and Fas-ligand (FasL),[18–22] we hypothesized that plm activation may control the cytokine storm and regulate the inflammatory response in murine models of aGVHD.

MATERIALS AND METHODS

Mice

Ten-week-old female C57BL/6 (B6; H-2^b) and six-week-old female (BALB/c × C57BL/6)F1 (CBF1; H-$2^{b/d}$) mice were purchased from Japan SLC Inc. (Hamamatsu, Japan). Ten-week-old female *Plg*$^{+/+}$ and *Plg*$^{-/-}$ mice, plasminogen activator inhibitor-1-deficient (*PAI1*$^{-/-}$) and *PAI1*$^{+/+}$ mice were used after more than 10 backcrosses onto C57BL/6 background. *Mmp9*$^{+/+}$ and *Mmp9*$^{-/-}$ mice were used after more than 10 backcrosses onto CD1 background. Animal protocols were approved by the Animal Review Board of The Institute of Medical Science, University of Tokyo.

Reagents

The plasmin inhibitor YO-2 [*trans*-4-aminomethylcyclohexanecarbonyl-Tyr(*O*-Pic)-octylamide] and YO-57 [*trans*-4-amiomethylcyclohexanecarbonyl-L-(*0*-picolyl)tyrosine-4-aminomethylanilide],[23,24] both provided by Yoshio Okada (Kobe Gakuin University, Kobe, Japan), were dissolved in

[1]Department of Stem Cell Regulation, Center for Stem Cell Biology and Regenerative Medicine, Institute of Medical Science at the University of Tokyo (IMSUT), Tokyo, Japan; [2]Department of Stem Cell Dynamics, Center for Stem Cell Biology and Regenerative Medicine, Institute of Medical Science at the University of Tokyo (IMSUT), Tokyo, Japan; [3]Department of Immunology, Atopy (Allergy) Research Center, Juntendo University School of Medicine, Tokyo, Japan; [4]Faculty of Pharmaceutical Sciences, Kobe Gakuin University, Kobe, Japan and [5]Department of Hematology and Oncology, Center for Stem Cell Biology and Regenerative Medicine, Tokyo, Japan. Correspondence: Dr K Hattori, Department of Stem Cell Regulation, Center for Stem Cell Biology and Regenerative Medicine, Institute of Medical Science at the University of Tokyo (IMSUT), 4-6-1, Shirokanedai, Minato-ku, Tokyo 108-8639, Japan.
E-mail: khattori@ims.u-tokyo.ac.jp
[6]These authors share senior authorship.
Received 21 November 2013; revised 1 April 2014; accepted 21 April 2014; accepted article preview online 5 May 2014; advance online publication, 3 June 2014

phosphate-buffered saline (PBS) at 375 μg/ml. The MMP inhibitor [N-hydroxy-2-((4-methoxysulfonyl)(3-pocolyl)-amino)-3- methylbutanamide (MMI270)] (Novartis Pharma Corporation, Basel, Switzerland)[25] was dissolved in dimethylsulfoxide at 10 mmol/l. The following reagents were used: D-(+)-galactosamine hydrochloride (GalN; Sigma-Aldrich, Tokyo, Japan), lipopolysaccharide (LPS; Sigma-Aldrich) from *Escherichia coli* 055:B5, mouse plg and plm (Innovative Research, Novi, MI, USA), recombinant human TNF-α (R&D Systems, Minneapolis, MN, USA).

Cell cultures

The human monocytic leukemia cell line THP-1 (3×10^5 cells/well) and the mouse monocytic leukemia cell line WEHI-274.1 (1×10^6 cells/well) were stimulated with 1 μg/ml LPS using 24-well Falcon plates (BD Biosciences, San Jose, CA, USA). A human FasL cDNA-transfected mouse T-lymphoma cell line (hFasL/L5178Y)[21,26] (1×10^6 cells/well) was cultured for 24 h.

Induction of lethal aGVHD

Bone marrow (BM) transplantation model: aGVHD was induced in lethally irradiated (8 Gy) CBF1 mice by intravenous injections of 1×10^7 BM cells and 5×10^7 splenocytes (SPs) from B6 mice on day 0. As a control, irradiated CBF1 mice were injected with the same number of BM cells and SPs from CBF1 mice. SP transfer model: CBF1 mice were intravenously injected with 2×10^8 SPs from B6 mice on day 0 and 7. Treatment: aGVHD mice were intraperitoneally injected with 3.75 mg/kg body weight (BW) of YO-2, YO-57 or PBS alone every day from days 0 to 28, day 0 to 14 or day 8 to 28.

Induction of lethal endotoxin shock

Mice were intraperitoneally injected with 400 mg/kg BW of GalN and 5 μg/kg BW of LPS (GalN/LPS). B6 mice were intraperitoneally injected with 3.75 mg/kg BW of YO-2 or PBS alone daily from day −5 to 2.

Enzyme-linked immunosorbent assay

Human TNF-α, FasL and plasmin inhibitor complex (PIC) were assayed in supernatants using commercial ELISA (enzyme-linked immunosorbent assay) kits (R&D Systems). Murine samples were assayed for TNF-α, IL-1β, FasL, MMP-9, IFN-γ, IL-6, MCP-1, plasmin-α2 antiplasmin complexes (PAP), uPA and tPA using ELISA kits (R&D Systems, BioLegend (San Diego, CA, USA), CUSABIO BIOTECH (Wuhan, China), Oxford Biomedical Research (Rochester Hills, MI, USA)).

aGVHD histopathology scoring

Tissues were fixed in 10% buffered formalin and embedded in paraffin. Hematoxylin and eosin stained tissue sections were evaluated using an OLYMPUS microscope and scored according to a published histopathological scoring system.[27] Standard magnifications were × 100/0.40 NA and × 200/0.75 NA.

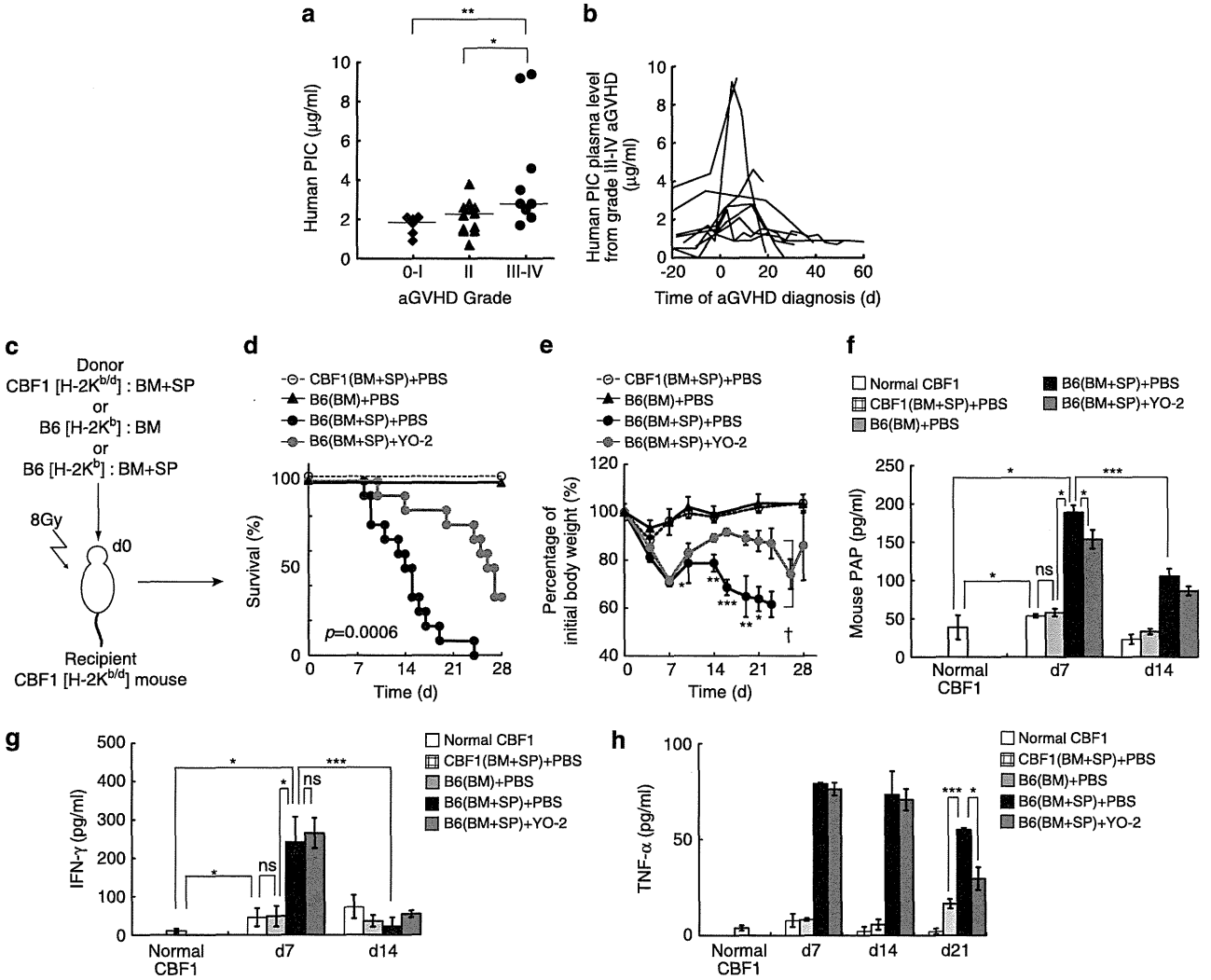

Figure 1. Plm is activated during the early phase of aGVHD. (**a**) ELISA of human PIC in plasma samples from human allo-HSCT recipients. (**b**) Human PIC plasma levels of patients with grade III–IV were plotted with day 0 set as the time of aGVHD onset. (**c–f**) aGVHD was induced in mice using a murine BM transplantation model. Mice were treated with PBS or YO-2 ($n = 12$/group). (**c**) Kaplan–Meier curves showing survival and (**e**) body weight. (**f**) ELISA of murine PAP ($n = 5$–11), (**g**) TNF-α ($n = 3$), and (**h**) IFN-γ ($n = 3$) in plasma at indicated times. Data represent mean ± s.e.m. from three independent experiments. $^*P < 0.05$, $^{**}P < 0.01$, $^{***}P < 0.001$.

© 2015 Macmillan Publishers Limited

Immunohistochemistry

Frozen murine tissue sections (5 μm) were washed with PBS, serum blocked and stained with the first antibody (Ab), overnight at 4 °C. Small intestine sections were stained with anti-CD11b Ab (1:50, clone M1/70; BD) followed by biotin-conjugated goat anti-rat IgG (1:200, CEDARLANW) and FITC-conjugated streptavidin (1:200, BD PharMingen, San Diego, CA, USA). Small intestine sections were stained with anti-CD3e Ab (1:50, BD PharMingen) followed by FITC-conjugate goat anti-armenian hamster IgG (H + L) (1:200, Abcam, Cambridge, MA, USA). Spleen sections were stained rabbit anti-murine MCP-1 (1:500, clone JE; PEPROTECH, Rocky Hill, NJ, USA)

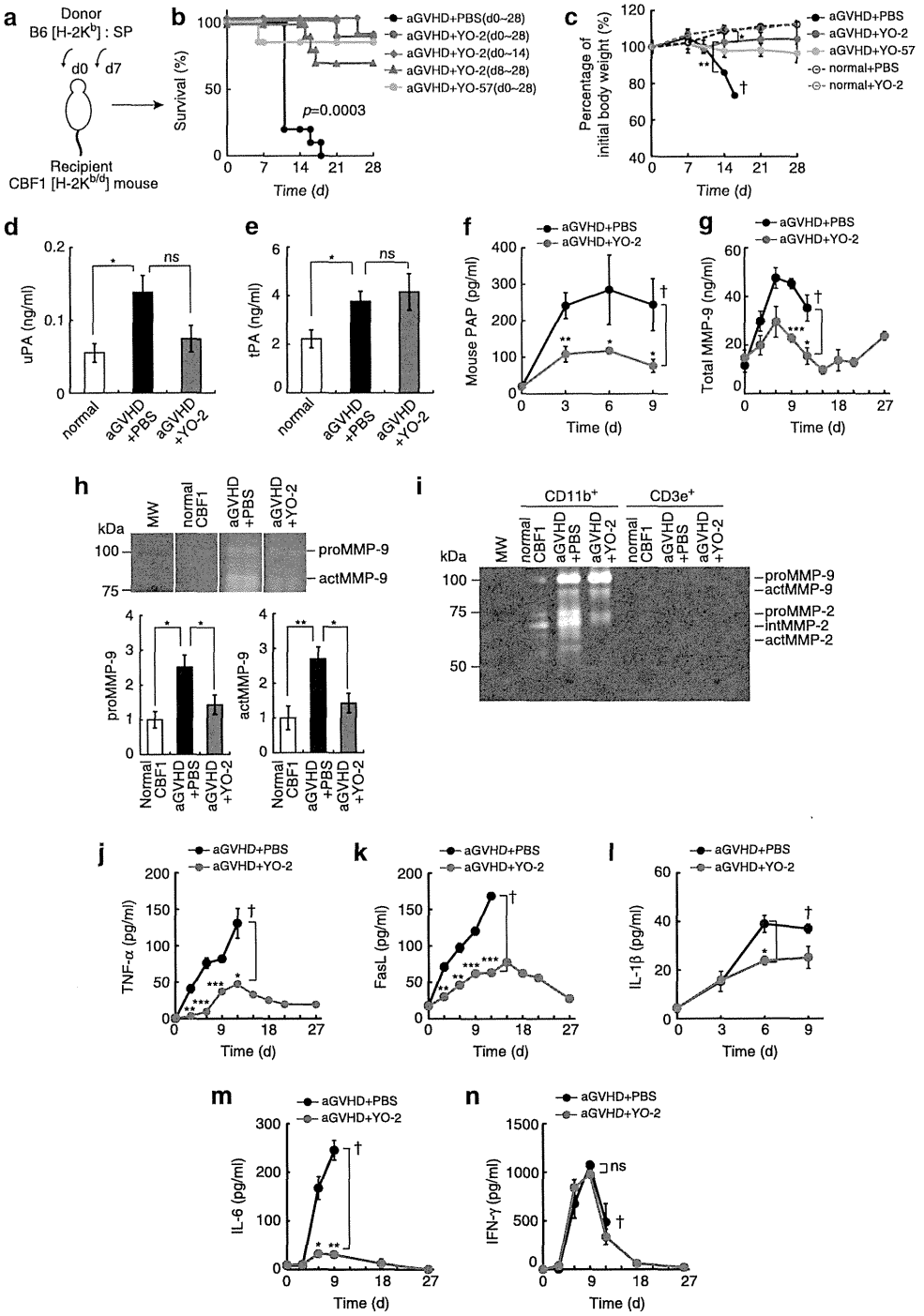

Figure 2. Plm inhibition protects against aGVHD-associated lethality by controlling proinflammatory cytokine/chemokine production. (**a**–**m**) aGVHD was induced in mice using a splenocytes (SPs) transfer model. Mice ($n = 10$/group) were treated with PBS, YO-2 and YO-57. Kaplan–Meier curves showing (**b**) survival and (**c**) body weight. ELISA of (**d**) uPA ($n = 3$) and (**e**) tPA ($n = 3$) in pooled plasma samples of three PBS- or YO-2-treated SP transfer model mice obtained at day 6. (**f**) Mouse PAP ($n = 7$–9) and (**g**) total MMP-9 ($n = 3$) were measured in plasma by ELISA. (**h**) Blood samples retrieved on day 6 were analyzed by gelatin zymography (upper panel). Quantification of the intensity of proMMP-9 and actMMP-9 bands (lower panel) ($n = 3$–4). (**i**) CD11b or CD3e positive FACS-sorted SPs from aGVHD mice at day 8 were cultured for 24 h. Culture supernatants were analyzed by gelatin zymography. (**j**) TNF-α, (**k**) FasL, (**l**) IL-1β, (**m**) IL-6 and (**n**) IFN-γ was measured by ELISA at indicated times in pooled plasma samples of PBS-and YO-2-treated aGVHD mice ($n = 3$/cytokines). Data represent mean ± s.e.m. from three independent experiments. $^*P < 0.05$, $^{**}P < 0.01$, $^{***}P < 0.001$. †Due to death no data available.

© 2015 Macmillan Publishers Limited

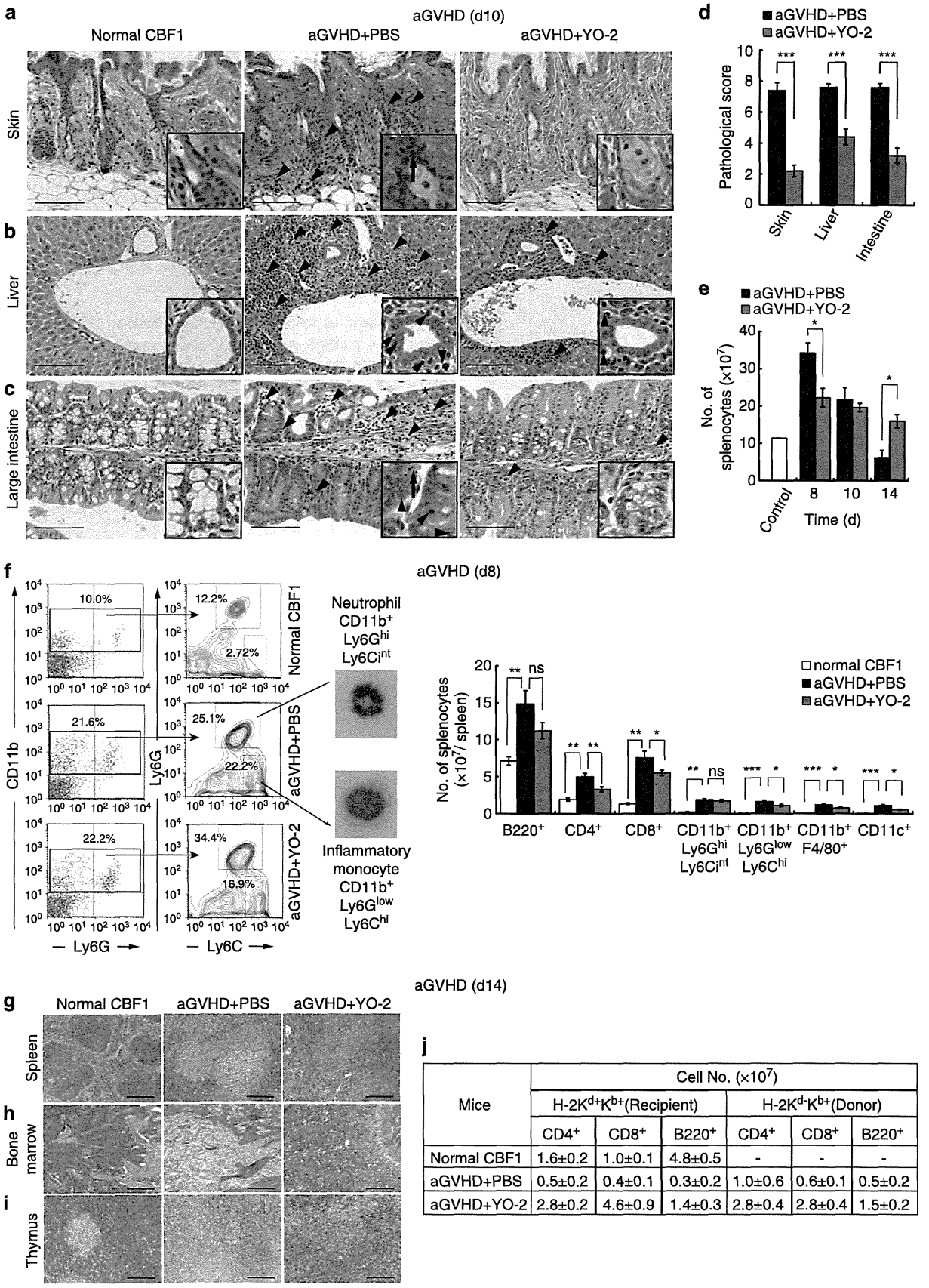

j

Mice	Cell No. (×10^7)					
	H-2K^d+K^b+(Recipient)			H-2K^d-K^b+(Donor)		
	CD4+	CD8+	B220+	CD4+	CD8+	B220+
Normal CBF1	1.6±0.2	1.0±0.1	4.8±0.5	-	-	-
aGVHD+PBS	0.5±0.2	0.4±0.1	0.3±0.2	1.0±0.6	0.6±0.1	0.5±0.2
aGVHD+YO-2	2.8±0.2	4.6±0.9	1.4±0.3	2.8±0.4	2.8±0.4	1.5±0.2

© 2015 Macmillan Publishers Limited

followed by Alexa Fluor 594 goat anti-rabbit IgG (H + L) (1:200, Invitrogen, Carlsbad, CA, USA), and costained with anti-CD31 Ab (1:500, clone ER-MP12; BMA Biomedicals, Augst, Switzerland) and biotin-conjugated goat anti-rat IgG (1:200, CEDARLNW) and Alexa Fluor 488 streptavidin (1:200, Invitrogen), or costained with anti-actin Ab (1:500, clone 3F10; GeneTex, Irvine, CA, USA) followed by Alexa Fluor 488 goat anti-mouse IgG (H + L) (1:200, Invitrogen).

WEHI-274.1 cells, after preincubation with 1 μg/ml of LPS with PBS or YO-2 for 2 h, were washed. Then cells were fixed with 4% PFA/PBS on slides and permeabilized with 0.1% Triton X-100/PBS after 30 min. Following blocking using 10% goat serum in PBS for 30 min, cells were incubated using anti-NFκB p65 (1:100; Santa Cruz, Dallas, TX, USA; sc-109) for 1 h in PBS with 1% BSA, washed three times with PBS, and incubated for 1 h with Alexa 594-conjugated goat anti-rabbit Ab (1:100; Invitrogen) in PBS with 1% BSA. After another washing step, cells were mounted with aqueous mounting medium.

Flow cytometric analysis

Cell-surface antigen analysis was performed by staining with the following Abs: goat anti-mouse CCR2 (AbD Serotec), CD4-PE, CD8a-PE, Gr-1-PE, Ly6G-PE, CD11c-PE, CD8a-FITC, F4/80-FITC, Ly6C-FITC, H2K^{d}-FITC B-220-APC, CD11b-APC, CD3e-APC, H-2K^{b}-biotin and APC streptavidin (BD PharMingen). Cells (1×10^{6}) were analyzed on a BD FACS Calibur.

PCR with reverse transcription analysis

Total RNA was extracted using Trizol (Invitrogen), and cDNA was generated according to the manufacturer's protocols. Specific forward and reverse primers, respectively, were designed as follows: human *TNF-α*: (5′-ttctccttcc tgatcgtg-3′) and (5′-agggctgattagagagaggt-3′); human *FasL*: (5′-gagagtctac cagccagatg-3′) and (5′-caggacaattccataggtgt-3′); human *uPA*: (5′-ccctcctctc ctccagaagaa -3′) and (5′-gtagacgatgtagtcctccttc-3′); human *uPAR*: (5′-ggtga cgccttcagcatga-3′) and (5′-cccactgcggtactggacat-3′); human *GAPDH* control: (5′-tggtctcctctgacttcaac-3′) and (5′-ctgttgctgtagccaaattc-3′); mouse *TNF-α*: (5′-gccgatttgctatctcatac-3′) and (5′-ggtatatgggctcataccag-3′); and mouse *β-actin* control: (5′-tggaatcctgtggcatccatgaaac-3′) and (5′-taaaacgca gctcagtaacagtccg-3′). Gene expression levels were measured using an ABI Prism 7500 sequence detection system (Applied Biosystems, Carlsbad, CA, USA).

Western blotting

Cells were lysed in lysis buffer (Cell Signaling Technology, Danvers, MA, USA). Recombinant murine MCP-1 (JE/CCL2, PEPROTECH) 50 nM were preincubated with 25 μM YO-2, followed by 7.15 IU/ml plm stimulation. Culture supernatants were removed after 30 min. Lysates/supernatants were separated by 16% Tricine-SDS–polyacrylamide gel electrophoresis and transferred to a PVDF membrane.[28] Membranes were immunoblotted with anti-TNF-α (1:1000; Cell Signaling Technology) and anti-β-tubulin (1:2000; Sigma-Aldrich) followed by HRP-conjugated or alkaline phosphatase-conjugated secondary Ab (1:500; Nichirei Bioscience, Tokyo, Japan). Membranes were immunoblotted with anti-mouse MCP-1 Ab (0.2 μg/ml; PEPROTECH) followed by HRP-conjugated secondary Ab (1:500; Nichirei Bioscience). Membranes were incubated with ECL-Plus (GE Healthcare Life Sciences, Piscataway, NJ, USA), and the chemiluminescent signal was detected on a LAS4000 (Fujifilm) according to the manufacturer's instructions. The alkaline phosphatase signal was detected using a Histofine Kit (Nichirei Bioscience).

Transwell migration assay

SPs derived from SP transfer mouse aGVHD model were isolated on 8 days after the initial transplantation, stained with CD11b-PE and CD3e-APC, and placed in the upper well of a 24-well transmigration chamber at 0.5×10^{6} cells per 0.1 ml (Corning, New York, NY, USA). Cells migrated for 2 h at 37 °C towards: 10 nM MCP-1 (JE/CCL2, PEPROTECH), ± 1.43 IU/ml plm and ± 5 μM YO-2. Migrated CD11b^{+} and CD3e^{+} subpopulations were calculated from the total number of SPs recovered and the percentages of CD11b^{+} and CD3e^{+} cells determined by FACS.

Zymography

MMP activity of plasma samples and culture supernatants was determined by gelatin zymography.[29,30] Density of each lytic band was quantified using image analysis software (ImageJ).

Chromogenic assay for plasmin activity

The kinetics of active plasmin formation was followed by measuring the release of *p*-nitroaniline from a chromogenic substrate (D-Val-Leu-Lys *p*-nitroanilide dihydrochloride, Sigma), detected as a change in absorbance (Δ405 nm/min) using a multiwell plate reader.

Plasma samples from the patients following HSCT

From January 2009 to June 2011, 27 patients underwent HSCT at the IMSUT. In accordance with the Declaration of Helsinki, patients gave their informed consent. We have obtained approval from the Ethics Committee of the IMSUT.

Statistical analysis

Survival curves were plotted using Kaplan–Meier estimates. We used the log-rank test for analysis of survival data and the Mann–Whitney *U*-test for statistical analysis of clinical scores. Student's *t*-test was used for statistical analysis of remaining data. Data are presented as means ± s.e.m. $P<0.05$ was considered statistically significant.

RESULTS

Plm is activated during the early phase of aGVHD

To investigate whether activation of plasmin (plm) occurs after HSCT and is associated with aGVHD, we analyzed patient plasma samples of human HSCT recipients. Patient demographics were compared (Supplementary Table 1) and the aGVHD severity was rated on a scale of Grade 0–I, Grade II and Grade III–IV (severe aGVHD). As a measure of plm activation, human plasmin α2-PIC plasma levels (around 0–100 days after transplantation) were determined. Individual maximum human PIC plasma levels correlated with the grade of aGVHD (Figure 1a). Human PIC levels peaked within the first 2 weeks after aGVHD diagnosis (Figure 1b) in circulation, which was followed by a decrease in plasminogen (plg), and an increase in thrombin–antithrombin and plasminogen activator inhibitor-1-tPA complex (PAI-1-tPA complex; Supplementary Figure 1). The clinical data indicated that plasmin activation was observed during early phase of severe aGVHD in humans.

Next, we studied the effect of plm inhibition during aGVHD progression in a murine major histocompatibility complex (MHC)-mismatched BM transplantation model of lethal aGVHD. CBF1 recipients received total body irradiation as a conditioning regimen followed by the transplantation of BM cells with or without SPs (Figure 1c). By day 21, SPs were of donor origin and blood counts had recovered (data not shown). Pharmacological plm inhibition was achieved using the plm inhibitor YO-2.[23,24] YO-2 inhibits plm by blocking the catalytic site, and efficiently inhibits circulating plm (Supplementary Figure 2a). YO-2 treatment delayed disease progression, showing improved survival and attenuated weight loss in mice (Figures 1d and e). Clinical signs of

Figure 3. Plm inhibition reduces aGVHD-associated tissue destruction, inflammatory changes and lymphoid hypoplasia. (**a–d**) Tissue sections from mice 8 days after SP transfer were stained with hematoxylin and eosin (H&E; scale bar, 100 μm). Representative images (× 200) of (**a**) skin, (**b**) liver and (**c**) large intestinal tissue sections show aGVHD-associated cell infiltration (arrow head), apoptotic body (arrow) and ulceration (asterisk). (**d**) Semi-quantitative histopathological scoring of tissues ($n = 5$/group). (**e**) Absolute numbers of SPs from mice following SP transfer determined at indicated times ($n = 5$). Data are the mean ± s.e.m. from three independent experiments. $^{*}P<0.05$, $^{**}P<0.01$ and $^{***}P<0.001$. (**f**) Absolute number of SP subpopulations calculated after obtaining the percentage of these cell populations by FACS. Spleens were harvested from CBF1, and PBS- or YO-2-treated aGVHD mice on day 8 ($n = 3$–5). (**g–i**) Tissue sections from mice 14 days after SP transfer were stained with H&E (scale bar, 200 μm). Representative images (× 100) of (**g**) spleen, (**h**) bone marrow and (**i**) thymus sections. (**j**) After determination of the percentages of each subpopulation by three-color FACS, the absolute cell numbers of CD4^{+} T, CD8^{+} T and B220^{+} B cells of host (H-2K^{d+}K^{b+}) or donor (H-2K^{d-}K^{b+}) origin in SPs from CBF1, PBS-treated or YO-2-treated aGVHD mice on day 14 were calculated from the total numbers of SPs recovered ($n = 3$). Data are representative from three independent experiments.

© 2015 Macmillan Publishers Limited